Adrenal Neoplasms: Lessons from Adrenal Multidisciplinary Tumor Boards

Ryan Chung, MD • Joanie Garratt, MD* • Erick M. Remer, MD • Patrick Navin, MB BCh • Michael A. Blake, MB, BCh • Myles T. Taffel, MD • Caitlin E. Hackett, MD • Kedar G. Sharbidre, MD • Wendy Tu, MD, FRCPC • Gavin Low, MB, ChB, MPhil, MRCS, FRCR • Meredith Bara, MD • Benjamin W. Carney, MD, MS • Michael T. Corwin, MD • Michael J. Campbell, MD • James T. Lee, MD • Cortney Y. Lee, MD • Julie C. Dueber, MD • Mostafa A. Shehata, MD • Elaine M. Caoili, MD • Nicola Schieda, MD • Khaled M. Elsayes, MD*

Author affiliations, funding, and conflicts of interest are listed at the end of this article.
*R.C. and J.G. contributed equally to this work.

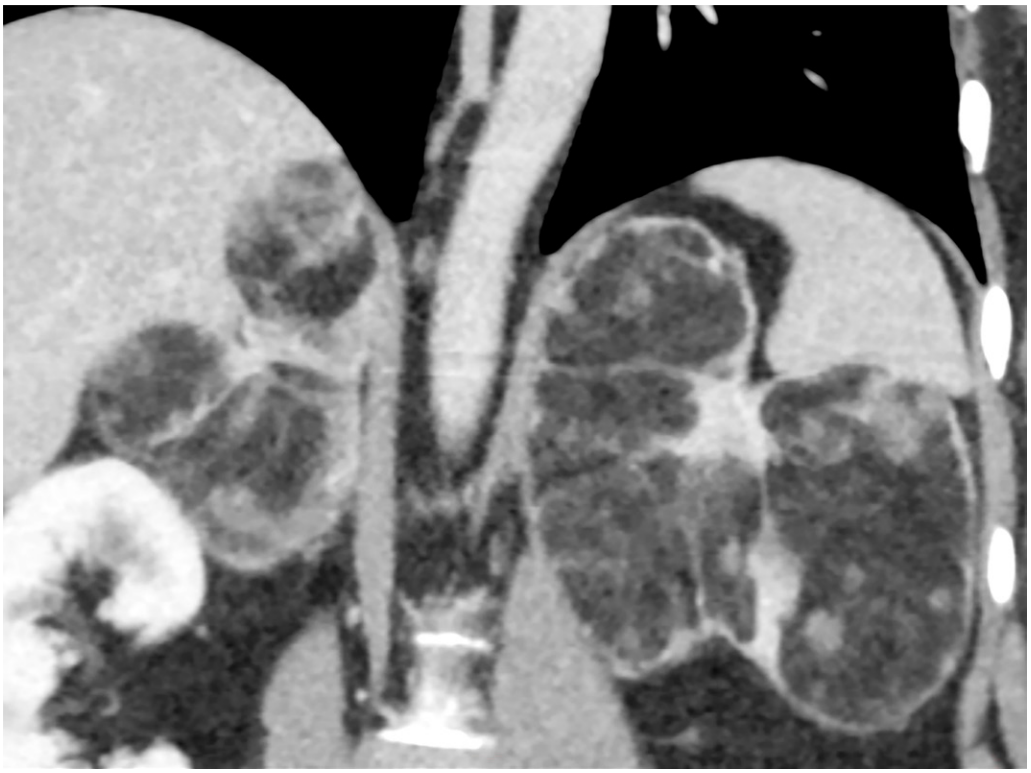

The radiologic diagnosis of adrenal disease can be challenging in settings of atypical presentations, mimics of benign and malignant adrenal masses, and rare adrenal anomalies. Misdiagnosis may lead to suboptimal management and adverse outcomes. Adrenal adenoma is the most common benign adrenal tumor that arises from the cortex, whereas adrenocortical carcinoma (ACC) is a rare malignant tumor of the cortex. Adrenal cyst and myelolipoma are other benign adrenal lesions and are characterized by their fluid and fat content, respectively. Pheochromocytoma is a rare neuroendocrine tumor of the adrenal medulla. Metastases to the adrenal glands are the most common malignant adrenal tumors. While many of these masses have classic imaging appearances, considerable overlap exists between benign and malignant lesions and can pose a diagnostic challenge. Atypical adrenal adenomas include those that are lipid poor; contain macroscopic fat, hemorrhage, and/or iron; are heterogeneous and/or large; and demonstrate growth. Heterogeneous adrenal adenomas may mimic ACC, metastasis, or pheochromocytoma, particularly when they are 4 cm or larger, whereas smaller versions of ACC, metastasis, and pheochromocytoma and those with washout greater than 60% may mimic adenoma. Because of its nonenhanced CT attenuation of less than or equal to 10 HU, a lipid-rich adrenal adenoma may be mimicked by a benign adrenal cyst, or it may be mimicked by a tumor with central cystic and/or necrotic change such as ACC, pheochromocytoma, or metastasis. Rare adrenal tumors such as hemangioma, ganglioneuroma, and oncocytoma also may mimic adrenal adenoma, ACC, metastasis, and pheochromocytoma. The authors describe cases of adrenal neoplasms that they have encountered in clinical practice and presented to adrenal multidisciplinary tumor boards. Key lessons to aid in diagnosis and further guide appropriate management are provided.

Supplemental Material

Quiz questions for this article are available through the Online Learning Center.

RadioGraphics 2023; 43(7):e220191
https://doi.org/10.1148/rg.220191

Content Codes: CT, GU, MR

Abbreviations: ACC = adrenocortical carcinoma, ACTH = adrenocorticotropic hormone, FDG = fluorine 18 fluorodeoxyglucose, HCC = hepatocellular carcinoma, RCC = renal cell carcinoma

TEACHING POINTS

- More recent data have shown that these values are not as specific for adenoma as previously believed, since other adrenal tumors such as pheochromocytoma, hypervascular metastases, and ACC also can meet these washout thresholds. Other features such as mass size, heterogeneity, and clinical context (eg, history of hypervascular malignancy or suspicion for pheochromocytoma) must be taken into account when using washout CT.
- Lipomatous and myelolipomatous degeneration occurs in primary adrenal tumors such as adenoma and rarely ACC. It is much less common than adrenal myelolipomas, which have a reported prevalence of up to 6%. At imaging, these areas of degeneration manifest as foci of macroscopic fat within an adrenal lesion, but they comprise a small percentage of the nodule (mean, 14% of the tumor in one series).
- In a relatively recent study, nearly one-third of adenomas grew over time, all at a rate of less than 3 mm per year, as compared with all malignant nodules, which grew at a rate of greater than 5 mm per year. A growth rate of less than 3 mm per year distinguished the adenomas from the malignant nodules with a sensitivity and specificity of 100%.
- Because the attenuation of simple fluid is less than or equal to 10 HU, a homogeneous unilocular cystic adrenal lesion can mimic adenoma at nonenhanced CT. Owing to their central hypoattenuation, cysts and pseudocysts may also mimic pheochromocytomas with cystic and/or necrotic change. A key feature of an adrenal cyst is its lack of enhancement.
- Multiple prior studies have shown that between 17% and 67% of pheochromocytomas demonstrate an absolute washout of greater than or equal to 60% and a relative washout of greater than or equal to 40%. A nonenhanced CT attenuation of less than or equal to 10 HU in the solid portion of the tumor is highly specific for adenoma, rarely occurring in pheochromocytoma. In addition, pheochromocytoma is characteristically hypervascular, manifesting as hyperenhancement during the portal venous phase.

Introduction

Adrenal tumors or tumor-like conditions are common in adults. An incidentally detected adrenal mass, or incidentaloma, is found in approximately 5% of imaging examinations performed for reasons not attributable to adrenal disease (1). In the absence of known malignancy, adrenal incidentalomas are overwhelmingly benign, with fewer than 1% of them representing malignancy (2,3). However, because the adrenal gland is a common site of metastasis and primary adrenal tumors other than benign nonhyperfunctioning adenomas do occur, correctly diagnosing these other entities can be challenging without an awareness of their common imaging appearances or when there is overlap in imaging features.

The American College of Radiology (ACR) white paper on incidental adrenal masses (1) recommends against pursuing any adrenal mass measuring less than 1 cm in short axis to avoid ambiguity regarding the possibility of a mass in the setting of nodularity or thickening and the potential for overdiagnosis and overtreatment of benign disease. In addition, the ACR white paper (1) provides guidance on the evaluation of adrenal masses based on their size, imaging features, and presence or absence of malignancy. When measuring the size of an adrenal mass, we recommend measuring its longest axis in any plane to determine management.

In this article, we discuss the common and atypical imaging appearances of adrenal adenoma, adrenocortical carcinoma (ACC), adrenal cyst, pheochromocytoma, myelolipoma, metastasis, bilateral adrenal disease, and select rare adrenal tumors and provide clues to the correct diagnosis. In addition, we highlight specific cases presented at multidisciplinary tumor boards and discuss the roles of different imaging modalities, biopsy, and surgery in select cases to further guide appropriate management.

Adrenal Adenoma

Adrenal adenoma is the most common adrenal tumor (4). Lipid-rich adenomas, accounting for approximately 70% of adrenal adenomas, contain microscopic fat, resulting in an attenuation value of less than or equal to 10 HU on conventional nonenhanced CT images when a region of interest is placed on the central two-thirds of a homogeneous lesion (5). The less than or equal to 10 HU threshold holds true for adrenal masses identified on virtual nonenhanced dual-energy CT images. Multiple studies (6–9) have shown that the attenuation on virtual nonenhanced images is higher than that on true nonenhanced images across dual-energy CT platforms, allowing the radiologist to be confident that an attenuation of less than or equal to 10 HU on virtual nonenhanced images is diagnostic of adenoma. However, this comes with a decrease in sensitivity for the detection of adenoma.

A lipid-rich adenoma demonstrates qualitative and quantitative loss of signal between in-phase and opposed-phase chemical shift imaging at MRI (10). There are multiple methods of calculating quantitative signal loss, with the simplest and most widely used method known as the adrenal signal intensity index, with which regions of interest are placed over the adrenal mass on the in-phase and opposed-phase MR images. The adrenal signal intensity index is a ratio and is defined as $[(SI_{in} - SI_{op})/SI_{in}] \times 100$, where SI_{in} is the in-phase signal intensity and SI_{op} is the opposed-phase signal intensity, with cutoff values of greater than 16.5% at 1.5 T and greater than 1.7% at 3 T diagnostic of adenoma (10). Fat-containing adrenal masses are summarized in Table 1.

In the absence of the above imaging features, long-term (≥12 months) stability of a solid adrenal mass or slow growth (≤3 mm/year) is most suggestive of a benign tumor, most commonly adenoma (1,11,12). The diagnosis of an adrenal adenoma can be challenging when typical imaging features are absent, and stability cannot be established. Atypical imaging features of adenomas include lipid-poor adenoma, macroscopic fat, hemorrhage, iron, heterogeneity, large size, and growth.

Lipid-Poor Adrenal Adenoma

An adenoma with a paucity or absence of microscopic fat has a nonenhanced CT attenuation of 10 HU or greater and is indeterminate. For some lipid-poor adenomas with a nonenhanced CT attenuation of 10–30 HU, MRI is useful for detecting microscopic fat on the basis of the signal loss on opposed-phase chemical shift MR images (13). However, MRI often does not show

Table 1: Adrenal Masses with Fat

Fat Type	Typical Masses	Atypical Masses	Tips
Microscopic fat	Adenoma	Fat-containing metastasis (eg, RCC, HCC)	Fat-containing extra-adrenal malignancy may be present; increased T2-weighted signal intensity and heterogeneity are suggestive of RCC metastasis rather than adenoma
		ACC	...
		Pheochromocytoma	...
Macroscopic fat	Myelolipoma	Adenoma with myelolipomatous degeneration	Consider biochemical testing for hypercortisolism for a mass with <50% macroscopic fat, as it may represent an adenoma
		ACC with myelolipomatous degeneration	...
		Extra-adrenal fat-containing mass (liposarcoma, RCC)	Identify organ of origin

Note.—HCC = hepatocellular carcinoma, RCC = renal cell carcinoma.

this signal loss when a lipid-poor adenoma has a nonenhanced CT attenuation of greater than 30 HU (Fig S1) (13–15). In this scenario, washout CT has generally been recommended to confirm adenoma in homogeneous nodules larger than 2 cm, and follow-up CT has been recommended for nodules 1–2 cm (1).

On nonenhanced, 60- to 90-second postcontrast portal venous phase, and 15-minute postcontrast delayed phase adrenal washout CT images, most adrenal adenomas demonstrate an absolute percentage washout of 60% or greater and a relative percentage washout of 40% or greater (16,17). Absolute percentage washout is defined as $[(HU_{pv} - HU_{dl})/(HU_{pv} - HU_{non})] \times 100$, and relative percentage washout is defined as $[(HU_{pv} - HU_{dl})/(HU_{pv})] \times 100$, where HU_{pv}, HU_{dl}, and HU_{non} are the attenuations during the portal venous, delayed, and nonenhanced phases, respectively (16). However, more recent data have shown that these values are not as specific for adenoma as previously believed, since other adrenal tumors such as pheochromocytoma, hypervascular metastases, and ACC also can meet these washout thresholds (18–20). Other features such as mass size, heterogeneity, and clinical context (eg, history of hypervascular malignancy or suspicion for pheochromocytoma) must be taken into account when using washout CT. Recent evidence has shown that the sensitivity of washout CT for an incidentally detected adrenal adenoma is lower than previously believed, ranging from 64% to 75% (18). In this instance, an adrenal mass that has been stable for 12 months or longer is most likely to be benign (1,11,12).

If stability cannot be confirmed and the patient has no history of malignancy, then the mass is still most likely to be benign (2,3), and follow-up CT in 6–12 months is suitable for an adrenal mass with indeterminate attenuation and washout characteristics. However, due to its relatively low sensitivity for incidental lesions, washout CT may best be used for distinguishing adenoma from metastasis in patients with a known history of nonhypervascular malignancy (21).

Metabolic imaging with fluorine 18 (^{18}F) fluorodeoxyglucose (FDG) PET/CT is both sensitive and specific for differentiating benign from malignant lesions (22,23). On FDG PET/CT images, adrenal adenoma is mildly FDG avid (22). Although higher mean and maximal standardized uptake value (SUV) (SUV_{mean} and SUV_{max}, respectively) measurements for an adrenal lesion are sensitive for malignancy, they are less specific because SUVs are susceptible to variability (22). Higher liver SUV ratio (adrenal lesion SUV_{max}:liver SUV_{mean}) values and the blood pool SUV ratio (adrenal lesion SUV_{max}: blood pool SUV_{mean}) are sensitive and specific for malignant adrenal lesions; a history of malignancy further increases specificity (23). Investigators in a relatively recent study (23) reported optimal liver SUV and blood pool SUV ratios of 2.5 and 3.4, respectively. Potential pitfalls include false-negative results for subcentimeter lesions, primary malignancies with low FDG avidity, and hemorrhagic or necrotic metastasis (22,23).

Adrenal Adenoma with Macroscopic Fat

On CT images, macroscopic fat has an attenuation of less than or equal to −20 HU. MRI shows loss of signal following the use of chemical selective fat-suppression sequences and India ink artifact at the interfaces between macroscopic fat and water on opposed-phase chemical shift images (24). Macroscopic fat within an adrenal mass is a classic feature of adrenal myelolipoma (25). However, the amount of fat within a myelolipoma can vary considerably, and small foci of macroscopic fat are not necessarily diagnostic of a myelolipoma. In some instances, they represent lipomatous or myelolipomatous degeneration within an adenoma (Fig 1) (26).

Lipomatous and myelolipomatous degeneration occurs in primary adrenal tumors such as adenoma and rarely ACC (24,26,27). It is much less common than adrenal myelolipomas, which have a reported prevalence of up to 6% (3). At imaging, these areas of degeneration manifest as foci of macroscopic fat within an adrenal lesion, but they comprise a small percentage of the nodule (mean, 14% of the tumor in one series) (26,28). Compared with myelolipoma, which is overwhelmingly nonfunctioning, myelolipomatous degeneration within an adrenal lesion has been suggested in some case series to possibly be associated with adrenal corticosteroid excess (26), although this requires validation in larger studies.

Adrenal Adenoma with Hemorrhage

Adrenal hemorrhage is most often unilateral, secondary to blunt trauma, or it may be bilateral, secondary to stress (eg, related to hypotension, sepsis, surgery, or burn), bleeding

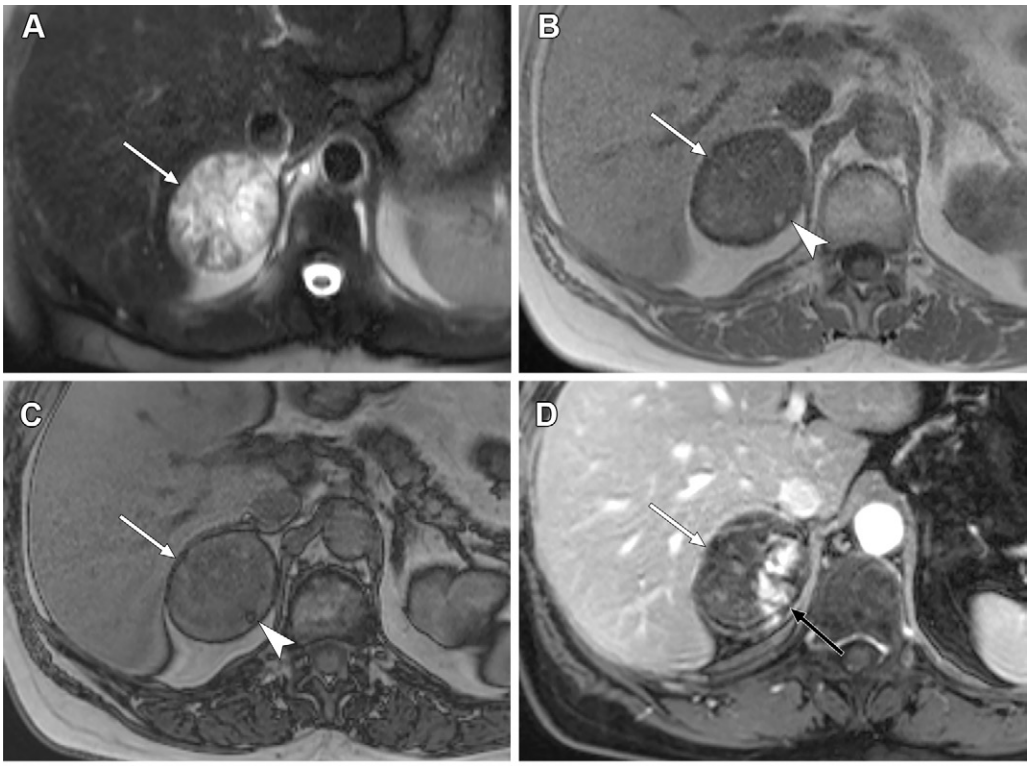

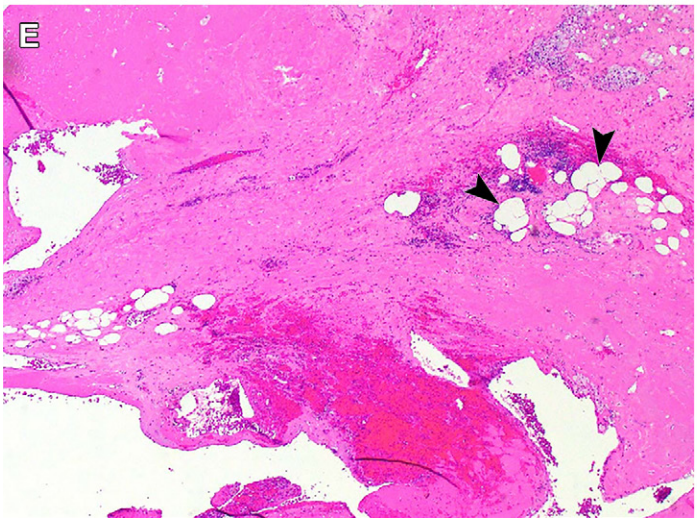

Figure 1. Incidental heterogeneously appearing right adrenal adenoma seen at lung cancer screening chest CT and further evaluated at MRI in a 62-year-old woman. **(A)** Axial T2-weighted MR image shows a 5.8-cm right adrenal mass (arrow) with a heterogeneous hyperintense signal. **(B, C)** Axial in-phase **(B)** and opposed-phase **(C)** chemical shift MR images show the mass (arrow), with a 4-mm rounded focus of T1 hyperintensity (arrowhead in **B**) posteriorly on the in-phase image and a surrounding rim of India ink artifact (arrowhead in **C**) on the opposed-phase image, compatible with macroscopic fat. No other areas of intralesional lipid are present. **(D)** Axial postcontrast T1-weighted MR image shows heterogeneous enhancement (black arrow) within the mass (white arrow). Because of its size, the mass was resected. **(E)** Low–power-field photomicrograph shows an adrenal adenoma with a 5-mm area of lipomatous degeneration (arrowheads) within an area of prior hemorrhage. (Hematoxylin-eosin stain; original magnification, ×40.)

diatheses, or hypercoagulable states (4). In addition, unilateral hemorrhage can occur within an adrenal mass (primary or metastatic); this may be difficult to identify during the acute presentation, which commonly involves abdominal pain.

Hemorrhage within an adrenal adenoma is uncommon but is suggested by interval enlargement of a previously characterized adenoma (Fig 2). CT generally shows heterogeneous enlargement, with areas of hemorrhage demonstrating hyperattenuation (50–90 HU) on nonenhanced images and no enhancement following contrast material administration (4,29). With dual-energy CT, areas of hemorrhage, as opposed to soft tissue within a mass, do not enhance between virtual nonenhanced images and postcontrast images or demonstrate uptake on iodine-enhanced images (30).

Hemorrhage depicted at MRI is age dependent, but it is generally recognizable as nonenhancing T1-hyperintense and T2-hypointense signal (4,29). Areas of hemorrhage can obscure enhancing soft tissue because of intrinsic T1-hyperintense signal. Subtraction images are key to identifying enhancing soft tissue that is diagnostic of an underlying mass with hemorrhage (4,29).

Identifying enhancing soft tissue can be challenging in the acute setting. Furthermore, rapid or marked enlargement of an adrenal mass due to hemorrhage can be difficult to distinguish from growth of a malignant mass. There are no established guidelines for follow-up to assess for an underlying mass after resolution of hemorrhage (31); however, follow-up imaging is often warranted, and 6–12 weeks after resolution of the hemorrhage is reasonable. Of note, mild elevation of plasma normetanephrine levels can occur secondary to hemorrhage and irritation of medullary cells (32). The adrenal masses that may have hemorrhage are summarized in Table 2.

Adenoma with Iron Deposition

Iron deposition within the reticuloendothelial system (eg, liver, spleen, and bone marrow) results in decreased signal intensity with all MRI pulse sequences, is most pronounced on T2*-weighted MR images, and demonstrates loss of signal on in-phase (sequence with the longer echo time) compared with opposed-phase MR images (33). Iron deposition can occur within a normal adrenal cortex following red blood cell transfusion and intravenous administration of ultrasmall superparamagnetic iron oxide particles (34). Iron deposition can also occur within an adrenal adenoma and result in signal loss with all MRI sequences, particularly on in-phase and opposed-phase chemical shift MR images (Fig 3) (20). This disrupts the typical signal loss at opposed-phase imaging that is

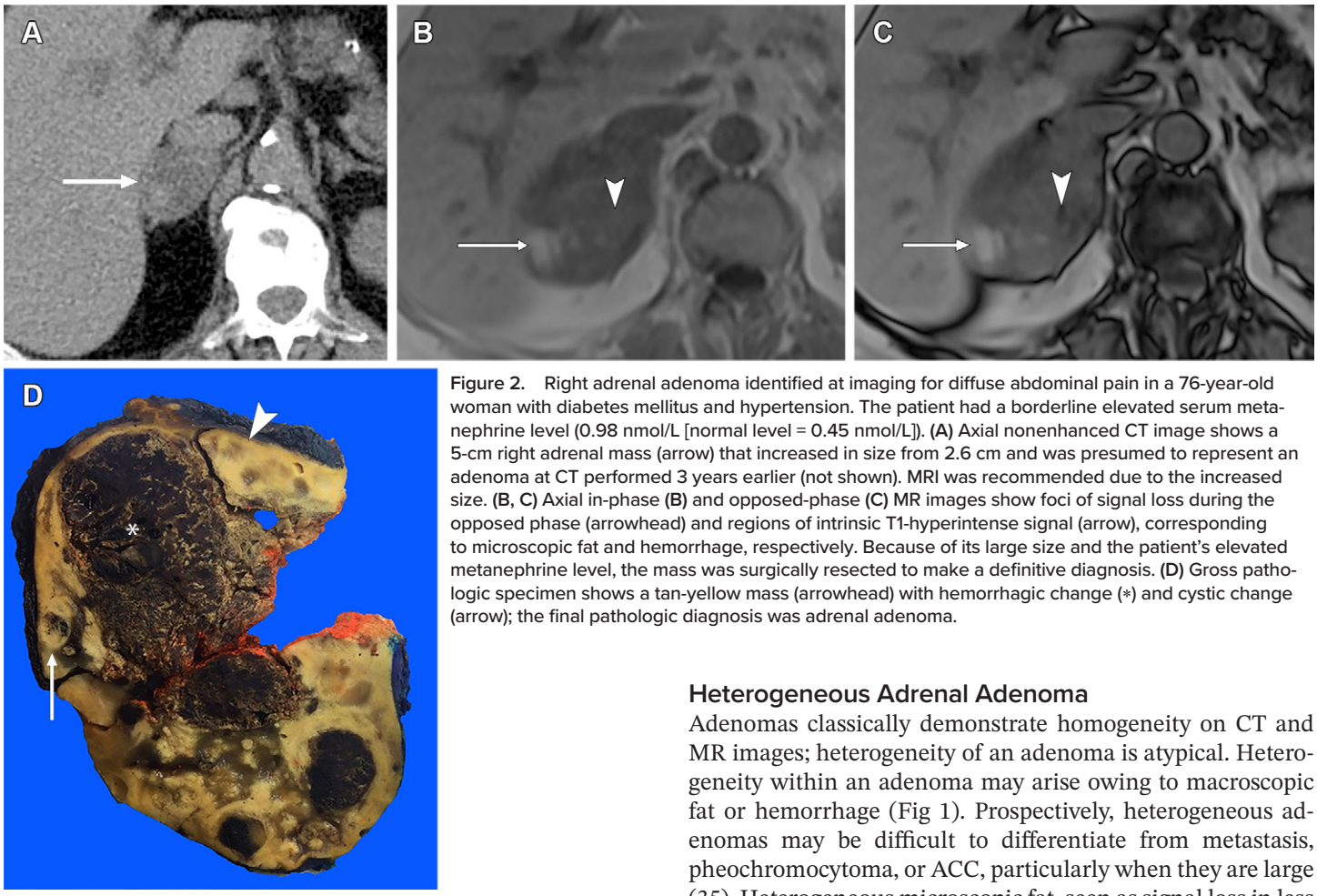

Figure 2. Right adrenal adenoma identified at imaging for diffuse abdominal pain in a 76-year-old woman with diabetes mellitus and hypertension. The patient had a borderline elevated serum metanephrine level (0.98 nmol/L [normal level = 0.45 nmol/L]). **(A)** Axial nonenhanced CT image shows a 5-cm right adrenal mass (arrow) that increased in size from 2.6 cm and was presumed to represent an adenoma at CT performed 3 years earlier (not shown). MRI was recommended due to the increased size. **(B, C)** Axial in-phase **(B)** and opposed-phase **(C)** MR images show foci of signal loss during the opposed phase (arrowhead) and regions of intrinsic T1-hyperintense signal (arrow), corresponding to microscopic fat and hemorrhage, respectively. Because of its large size and the patient's elevated metanephrine level, the mass was surgically resected to make a definitive diagnosis. **(D)** Gross pathologic specimen shows a tan-yellow mass (arrowhead) with hemorrhagic change (*) and cystic change (arrow); the final pathologic diagnosis was adrenal adenoma.

Table 2: Adrenal Masses with Hemorrhage

Atypical masses
Pheochromocytoma (most common)
Metastasis
Adrenocortical carcinoma
Myelolipoma
Adenoma
Tips
Perform dual-energy CT or MRI to identify underlying mass
Perform follow-up imaging in 6–12 weeks to assess for underlying mass after hemorrhage has resolved
No adrenal masses typically have hemorrhage

characteristic of microscopic fat within an adenoma and may mimic chronic hemorrhage or calcifications. Prior imaging findings, the clinical history, and iron deposition in the reticuloendothelial system are important clues to the diagnosis. Adrenal washout CT may help identify an adenoma with iron deposition because the washout characteristics are not affected by iron deposition; however, to our knowledge, this has not been demonstrated.

Heterogeneous Adrenal Adenoma

Adenomas classically demonstrate homogeneity on CT and MR images; heterogeneity of an adenoma is atypical. Heterogeneity within an adenoma may arise owing to macroscopic fat or hemorrhage (Fig 1). Prospectively, heterogeneous adenomas may be difficult to differentiate from metastasis, pheochromocytoma, or ACC, particularly when they are large (35). Heterogeneous microscopic fat, seen as signal loss in less than 80% of the mass at opposed-phase chemical shift MRI, indicates a high likelihood of benignancy in patients without prior cancer. This also holds true for adrenal nodules in patients with most malignancies. However, the radiologist should be cautious in the setting of patients with fat-containing malignancies such as hepatocellular carcinoma (HCC) and renal cell carcinoma (RCC) or when the morphologic pattern of signal loss is suggestive of a collision tumor (with two distinct parts or peripheral signal loss) (35). It is reasonable to perform short-interval follow-up CT to demonstrate stability that supports a benign lesion.

Large Adrenal Adenoma

A 4-cm or larger adrenal adenoma is atypical, but it often has imaging features that are seen in smaller adenomas, including homogeneity and well-circumscribed margins without local invasion (36). However, a 4-cm or larger adrenal mass has a higher rate of malignancy than a mass smaller than 4 cm (4,37). A 4-cm threshold is sensitive (up to 93%) but less specific for malignancy than a 6-cm cutoff (38). In one study involving 705 adrenal tumors (39), the prevalence of malignancy in adrenal lesions larger than 4 cm was 31%, and the risk of malignancy increased proportionally with tumor size. However, malignancy cannot be determined by size alone; older age at diagnosis and higher attenuation at nonenhanced CT (>20 HU) are additional predictors of malignancy (39). In addition, ACC is often heterogeneous with cystic and/or necrotic

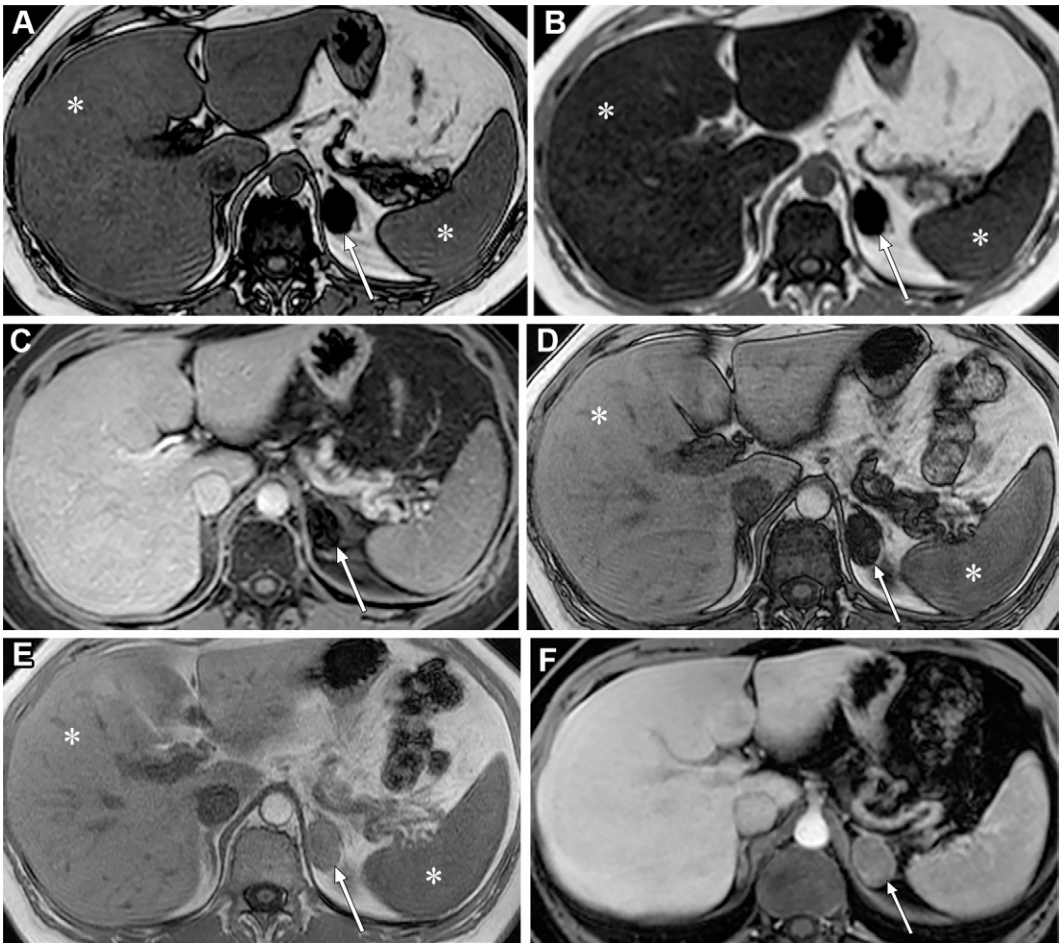

Figure 3. Left adrenal adenoma in a 39-year-old woman with breast cancer and diffuse hepatic iron deposition that was seen as liver and spleen (* in **A**, **B**, **D**, **E**) signal loss on an initial in-phase MR image **(B)**. **(A–C)** Initial contrast-enhanced MR images obtained for evaluation of a liver lesion (not shown) during the opposed phase **(A)**, in phase **(B)**, and postcontrast portal venous phase **(C)** show a left adrenal nodule (arrow) with hypointensity that was unchanged between the opposed **(A)** and in **(B)** phases. Postcontrast portal venous phase image **(C)** shows diffuse low signal intensity in the nodule, which was interpreted as an incidental calcified nodule or a remote left adrenal hematoma. **(D–F)** Axial 6-month follow-up opposed-phase **(D)**, in-phase **(E)**, and postcontrast portal venous phase **(F)** MR images show the left adrenal nodule (arrow), with the previously identified diffuse signal loss in the liver and spleen during the in phase, relative to the opposed phase, no longer present. There is stable size of the left adrenal nodule, which now shows diffuse signal loss during the opposed phase, compatible with microscopic fat and homogeneous postcontrast enhancement, findings that are consistent with adrenal adenoma. The imaging features of the adrenal lesion seen at initial MRI were due to iron deposition in the adenoma.

change, hemorrhage, or invasion of adjacent organs or veins, and nearly 70% of ACCs are 6 cm or larger (4,37).

It may be impossible to distinguish a large atypical adenoma from an ACC or other malignant mass with imaging because of overlapping imaging features. If there are no benign diagnostic features, evaluation of the clinical context, including hormonal assessment, is essential for assessing the need for surgical resection of a 4-cm or larger adrenal mass (Fig 1) (39). Patients with a large adrenal mass should be managed by a multidisciplinary team that includes surgeons, endocrinologists, and radiologists (39).

Slow Growth of Adenoma

Stable size of an adrenal mass for 12 months or longer is suggestive of benignity, whereas significant growth is suggestive of malignancy (1,11,12). Because adrenal adenoma is overwhelmingly the most common benign adrenal neoplasm, it is the presumed diagnosis in cases of a stable adrenal mass (40). Conversely, growth of an adrenal mass is suspicious for a nonadenoma. However, in a relatively recent study (11), nearly one-third of adenomas grew over time, all at a rate of less than 3 mm per year, as compared with all malignant nodules, which grew at a rate of greater than 5 mm per year. A growth rate of less than 3 mm per year distinguished the adenomas from the malignant nodules with a sensitivity and specificity of 100% (Fig S2) (11). The growth rates of adrenal masses are summarized in Table 3.

Adrenocortical Carcinoma

ACC is a rare malignant tumor of the adrenal cortex with a bimodal distribution, affecting children younger than 5 years and adults in their 4th to 5th decade of life (37). Patients may present with abdominal pain, distention, or a palpable mass. ACC may produce excess cortisol, androgen, estrogen, or aldosterone levels, although hormonal excess may be absent (39).

ACC is typically a large circumscribed mass with heterogeneous attenuation due to cystic and/or necrotic change, hemorrhage, and calcification (37,41). Smaller ACCs may be homogeneous and difficult to distinguish from adenomas, particularly if they are smaller than 4 cm. On nonenhanced CT images, ACC rarely has an attenuation lower than 20 HU, which helps differentiate it from adenoma (2). ACC enhances heterogeneously, with areas of central nonenhancement due to necrosis or hemorrhage (37,41). Although data are limited, ACC often shows an absolute washout of less than 60%, but it may exceed washout thresholds that are compatible with adenoma (Fig S3) (37,41).

On MR images, ACC demonstrates heterogeneous signal intensity with variable amounts of nonenhancing central T2-hyperintense signal (cystic and/or necrotic change) and intrinsic T1-hyperintense signal (hemorrhage) (42,43).

On both CT and MR images, a 4-cm or larger adrenal mass increases the likelihood of ACC, with up to 70% of ACCs presenting as a 6-cm or larger mass (37). Kahramangil

Table 3: Growth Rates of Typical and Atypical Adrenal Masses

Growth Rate	Typical Masses	Atypical Masses	Tips
<3 mm/y	Adenoma, myelolipoma, cyst or pseudocyst	Not applicable	Adenomas can grow up to 3 mm/year
>5 mm/y	Metastasis, ACC, pheochromocytoma	Myelolipoma (in the setting of congenital adrenal hyperplasia and medication nonadherence)	Malignancies tend to grow 5 mm or more per year; rapid growth can cause or result from acute hemorrhage

Table 4: Adrenal Masses with Cystic and/or Necrotic Change

Typical Masses	Tips
Cyst	Perform adrenal washout CT, dual-energy CT, or gadolinium-enhanced MRI to assess for enhancement
Metastasis	Masses should be suspected in the presence of extra-adrenal malignancy, new or rapid growth of an adrenal mass, multiple adrenal masses, or other metastases
Pheochromocytoma (common)	Perform biochemical evaluation for adrenal mass <4 cm with cystic and/or necrotic change and hyperenhancement, even if absolute washout is ≥ 60%, because these features are common in pheochromocytoma; look for a thickened rind of enhancing soft tissue to distinguish cyst from cystic and/or necrotic change
ACC	

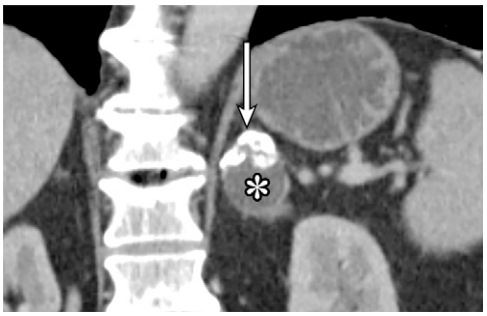

Figure 4. Left adrenal pseudocyst in a 63-year-old man. Coronal portal venous phase CT image shows a 3.6-cm left adrenal mass (*) that has homogeneous simple fluid attenuation with coarse peripheral calcifications (arrow). The mass was stable for 3 years, and abdominal MRI findings (not shown) confirmed the presence of internal cystic contents and the absence of enhancing soft tissue.

et al (2) reported an ACC prevalence of 1.7% among 2219 adrenal incidentalomas, with ACC rates by size of 0.1%, 2.4%, and 19.5% for adrenal incidentalomas smaller than 4 cm, 4–6 cm, and 6 cm or larger, respectively. Another group of authors (44) reported prevalences of 0.2%, 4.8%, and 37.7%, respectively, in their cohort of 2498 adrenal incidentalomas, in which 18 of 214 resected tumors were ACCs. Additional clues to the diagnosis of ACC include irregular margins, local invasion of adjacent organs, venous invasion or tumor thrombus, and metastases. The adrenal masses with cystic and/or necrotic change are summarized in Table 4.

ACC rarely contains microscopic fat (45) or macroscopic fat (37,41,46). ACC with macroscopic fat usually occurs in a mass larger than 6 cm that is heterogeneous and invasive, with macroscopic fat comprising less than 5% of the mass (46). Furthermore, patients are often symptomatic, or there are other factors that herald the correct diagnosis (46).

ACC is an FDG-avid tumor, and FDG PET/CT may help in identifying the primary tumor or evaluating for local recurrence or metastasis (42). The role of biopsy for indeterminate adrenal lesions is controversial. Percutaneous biopsy of ACC in particular is often avoided because of the risk of tumor seeding along the needle track, capsule breakdown, and difficulty reliably distinguishing ACC from adenoma in biopsy specimens (21). However, the benefits of biopsy may exceed the risks in patients who are poor surgical candidates (37).

Adrenal Cyst

Adrenal cyst is a differential diagnosis for a low-attenuation (0–20-HU) adrenal lesion (Fig S2). There are four types of adrenal cysts: endothelial-vascular, pseudocyst, epithelial, and parasitic (4). Endothelial cysts and pseudocysts make up more than 80% of all adrenal cysts (4). All adrenal cysts demonstrate simple fluid attenuation with varying degrees of loculation, septa, and calcification. Endothelial and epithelial cysts are usually thin walled and multilocular and can contain septal calcifications, whereas pseudocysts have a slightly thicker wall, are unilocular, and can contain peripheral calcifications (Fig 4). A pseudocyst arises from prior hemorrhage. Parasitic (echinococcal) cysts have the thickest walls, are unilocular or multilocular, and can contain peripheral calcifications and daughter cysts.

Because the attenuation of simple fluid is less than or equal to 10 HU, a homogeneous unilocular cystic adrenal lesion can mimic adenoma at nonenhanced CT. Owing to their central hypoattenuation, cysts and pseudocysts may also mimic pheochromocytomas with cystic and/or necrotic change. A key feature of an adrenal cyst is its lack of enhancement.

Figure 5. Right adrenal cyst in a 35-year-old man with urinary frequency. **(A)** Sagittal color Doppler abdominal US image shows a thin-walled anechoic mass (arrow) in the right retroperitoneum, with posterior acoustic enhancement and no internal nodularity or flow. The mass was interpreted as a small adrenal cyst or exophytic right renal cyst, and CT was recommended. **(B)** Axial nonenhanced CT image shows a circumscribed right adrenal nodule (arrow) with an attenuation of 15 HU that was interpreted as indeterminate for adenoma; MRI was recommended. **(C)** Axial T2-weighted MR image shows a homogeneously T2-hyperintense nodule (arrow) with signal intensity similar to that of cerebrospinal fluid and no microscopic fat at gradient-echo MRI or enhancement at postcontrast MRI (not shown). This case illustrates that cysts are included in the differential diagnosis for a homogeneous low-attenuation (0–20-HU) adrenal lesion and can be mistaken for adenoma. The combined US and CT findings were diagnostic for a cyst.

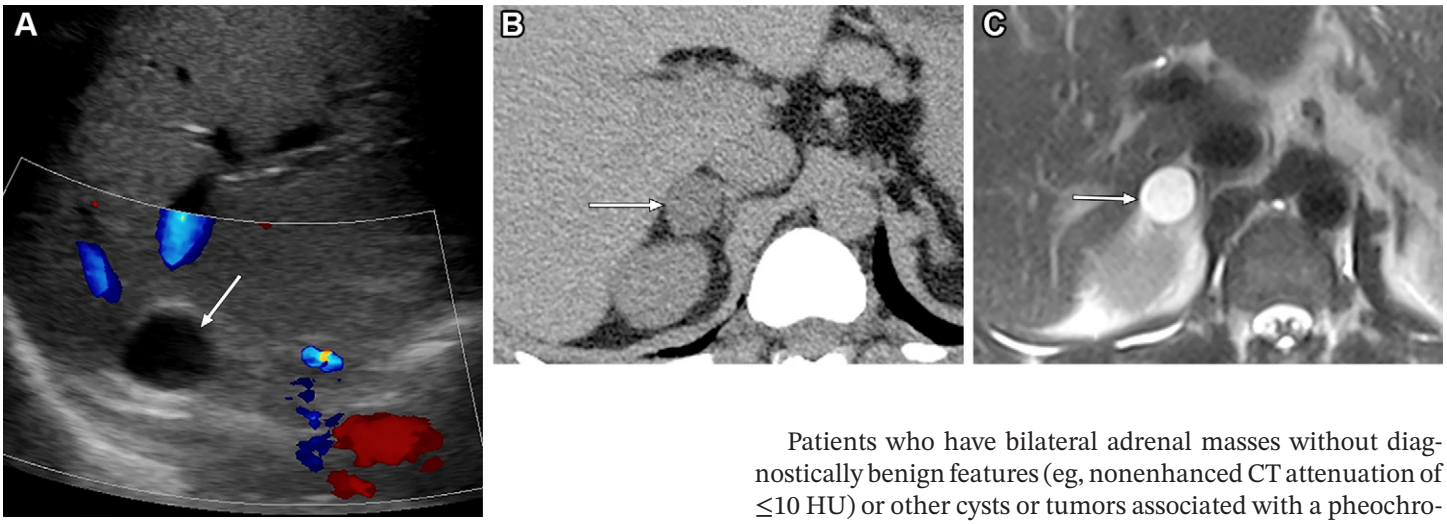

On US images, a cyst is anechoic with varying degrees of wall thickening, septation, and echogenic shadowing calcifications. With adrenal washout CT, one can easily distinguish a cyst from an adenoma, because an adenoma enhances while a cyst does not. MRI shows hyperintensity on T2-weighted images (Fig 5), hypointensity on T1-weighted images, and no enhancement on gadolinium-enhanced images. Macroscopic fat and microscopic fat are absent. There is a paucity of data on whether follow-up imaging is needed, and there are no guidelines for determining the frequency and duration of follow-up imaging (47,48).

Pheochromocytoma

Pheochromocytoma is a rare catecholamine-secreting neuroendocrine tumor that develops from the chromaffin cells of the adrenal medulla, and it occurs most often in middle-aged adults. As most pheochromocytomas are hormonally active, patients may present with symptoms such as palpitations, headache, diaphoresis, and signs of hypertension (49). However, these tumors are incidentally diagnosed with imaging, accounting for up to 3%–5% of adrenal incidentalomas (10,21,43).

Although most pheochromocytomas develop sporadically, approximately one-third of them are associated with germline mutations (19). Compared with sporadic pheochromocytoma, hereditary pheochromocytoma is more often asymptomatic and associated with lower 24-hour urinary normetanephrine levels, smaller size at detection, and detection in younger patients (19).

A suspected diagnosis of pheochromocytoma must be confirmed with biochemical testing, including analysis of elevated plasma or 24-hour urine fractionated metanephrine levels (43,49). Biopsy is not recommended; instead, surgical resection is required to avoid the sequelae from excess catecholamine levels (21,43).

Patients who have bilateral adrenal masses without diagnostically benign features (eg, nonenhanced CT attenuation of ≤10 HU) or other cysts or tumors associated with a pheochromocytoma syndrome should be evaluated with biochemical testing for pheochromocytoma (Fig 6). This workup should be performed regardless of whether the adrenal masses demonstrate washout consistent with adenoma, as pheochromocytoma may meet these thresholds.

At MRI, approximately two-thirds of pheochromocytomas show increased signal intensity, described as being "light-bulb bright," on T2-weighted images (20). This imaging feature overlaps with the T2 hyperintensity from cystic changes in adenomas and pheochromocytomas. Use of the quantitative T2-weighted signal intensity ratio has been shown to improve sensitivity and specificity in differentiating pheochromocytoma from other lesions (20,50). For instance, Borhani and Hosseinzadeh (50) reported that an adrenal-to-muscle signal intensity ratio of at least 3.95 at 1.5-T MRI was 81% sensitive and 88% specific for diagnosing pheochromocytoma.

Between 22% and 97% of pheochromocytomas demonstrate cystic and/or necrotic change (19,21,51). *Cystic and/or necrotic change* is defined as a focal central area of low attenuation subjectively similar to fluid attenuation within a solid mass or nodule on CT images and hyperintense signal on T2-weighted MR images, without corresponding enhancement. It is an imaging appearance, but it does not imply a pathologic diagnosis of necrosis (52). On images, the distinguishing feature of pheochromocytoma with a cystic and/or necrotic appearance is a thick enhancing wall that retains contrast enhancement on delayed postcontrast images (Fig 7) (49); septa may or may not be present (52). In the case of an incidental solid adrenal mass with cystic and/or necrotic change, pheochromocytoma should be strongly considered (21). Laboratory evaluation is recommended to confirm the diagnosis.

A large pheochromocytoma can exert mass effect or invade adjacent structures; this may make distinguishing pheochromocytoma from ACC difficult, as cystic and/or necrotic change, heterogeneity, and enhancement can be seen in both of these tumors (Fig 8). Metastases can occur with

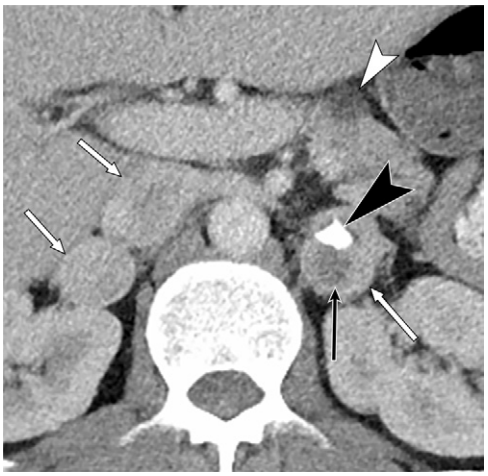

Figure 6. Bilateral pheochromocytoma in a 38-year-old man with von Hippel–Lindau syndrome. Axial contrast-enhanced portal venous phase CT image shows two right and one left heterogeneously enhancing adrenal nodules (white arrows) with cystic change (black arrow) and calcification (black arrowhead) in the left adrenal nodule. A pancreatic tail cyst (white arrowhead) and enhancing pancreatic body mass (not shown) also were present. Bilateral pheochromocytomas were confirmed at right adrenalectomy and partial left adrenalectomy.

both pheochromocytoma and ACC. It should be noted that all pheochromocytomas have metastatic potential, diagnosed on the basis of the presence of chromaffin cells at sites outside of their normal location (adrenal gland and sympathetic and parasympathetic ganglia) (53). Although both pheochromocytoma and ACC may develop sporadically, a predisposing hereditary mutation may favor one diagnosis over the other. Additional clues include elevated metanephrine levels (for pheochromocytoma) or elevations of other hormones such as cortisol, androgen, estrogen, and aldosterone (for ACC) (37).

Pheochromocytoma with Greater than 60% Contrast Material Washout

Multiple prior studies have shown that between 17% and 67% of pheochromocytomas demonstrate an absolute washout of greater than or equal to 60% and a relative washout of greater than or equal to 40% (Fig 9) (18–20,54,55). A nonenhanced CT attenuation of less than or equal to 10 HU in the solid portion of the tumor is highly specific for adenoma, rarely occurring in pheochromocytoma (19). In addition, pheochromocytoma is characteristically hypervascular, manifesting as hyperenhancement during the portal venous phase. Several portal venous phase attenuation thresholds to distinguish pheochromocytoma from adenoma have been studied: greater than or equal to 130 HU was 38% sensitive and 100% specific (55), and greater than or equal to 85 HU was 88% sensitive and 84% specific (54). In addition to the aforementioned features, a proposed modified criterion to distinguish adenoma from pheochromocytoma includes one of the following: *(a)* lesion attenuation of greater than or equal to 40 HU at nonenhanced CT, *(b)* lesion attenuation of greater than or equal to 160 HU at portal venous phase CT, *(c)* lesion attenuation of greater than or equal to 70 HU at 15-minute delayed CT, or *(d)* intralesional cystic degeneration at portal venous phase CT and 15-minute delayed phase CT (56). We recommend biochemical testing for pheochromocytoma when an adrenal mass demonstrates cystic and/or necrotic change or has a portal venous phase CT attenuation of greater than or equal to 130 HU, even if the washout threshold is suggestive of adenoma.

If there is ongoing high clinical suspicion for pheochromocytoma despite negative biochemical testing results, molecular imaging with gallium 68 (^{68}Ga)–labeled somatostatin analogs (^{68}Ga-DOTA Phe1-Tyr^{3}-octreotide, ^{68}Ga–tetraazacyclododecane tetraacetic acid-octreotate, and ^{68}Ga-DOTA NaI^{3}-octreotide), ^{18}F-fluorodopamine, ^{18}F-fluorodihydroxyphenylalanine (^{18}F-DOPA), or ^{123}I-metaiodobenzylguanidine (^{123}I-MIBG) may confirm pheochromocytoma. Note that the reported sensitivities of ^{68}Ga-labeled somatostatin analogs are greater than those of ^{18}F-fluorodopamine and ^{18}F-DOPA, and the reported sensitivities of ^{18}F-fluorodopamine and ^{18}F-DOPA are greater than those of ^{123}I-MIBG (57). In addition to aiding in the diagnosis of pheochromocytoma in the setting of equivocal biochemical or anatomic imaging results, molecular imaging can be used to assess the local-regional extent of disease, identify tumor multiplicity and metastasis, and detect therapeutic molecular targets (57).

Pheochromocytoma with Hemorrhage

Hemorrhage is a rare complication; however, pheochromocytoma is the most common primary tumor to hemorrhage. Although the underlying mechanism of pheochromocytoma with hemorrhage is unknown, some theories suggest increased intracapsular pressure from trauma, a rapidly enlarging tumor that outgrows its blood supply, and vasodilatation and interstitial hemorrhage caused by the use of antihypertensive medications. Patients may present with symptoms of a hypertensive crisis secondary to excessive catecholamine release from a ruptured pheochromocytoma (43). Intratumoral hemorrhage manifests as increased attenuation of a pheochromocytoma on nonenhanced CT images or intrinsic T1-hyperintense signal on MR images (41). Bleeding and rupture of a pheochromocytoma may manifest as retroperitoneal hemorrhage (Fig 10). As mentioned earlier, adrenal hemorrhage from any cause may lead to transient metanephrine elevation (32).

Myelolipoma

Composed of adipose and hematopoietic tissue, myelolipoma is an uncommon benign neoplasm that is often hormonally inactive and mainly found in the adrenal glands (58). The prevalence of adrenal myelolipoma can be as high as 6% (3).

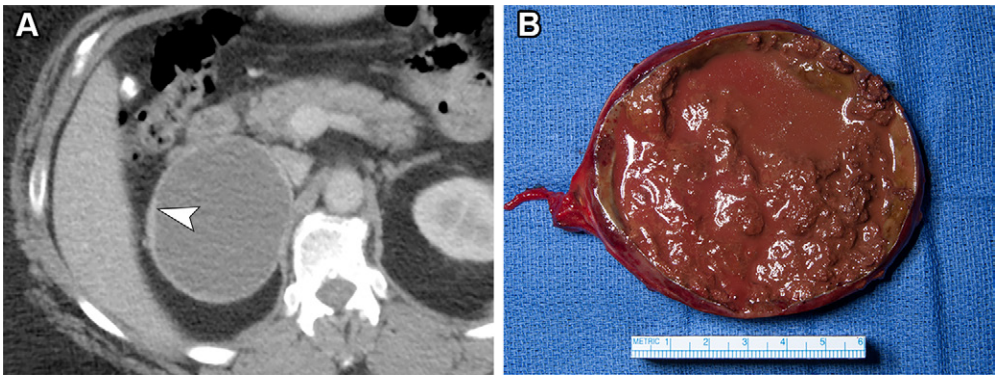

Figure 7. Incidentally found cystic pheochromocytoma in a 50-year-old woman with persistent hypertension who presented with acute abdominal pain and emesis. **(A)** Axial portal venous phase CT image shows a markedly enhancing rim of soft tissue (105 HU) (arrowhead). Endocrine workup revealed a urinary metanephrine level of 1022 mcg/24 h (normal level, <400 mcg/24 h) and a normetanephrine level of 6761 mcg/24 h (normal level, <900 mcg/24 h). **(B)** Gross pathologic specimen shows a well-circumscribed mass that was cystic, hemorrhagic, and necrotic at sectioning and contained red-brown friable material.

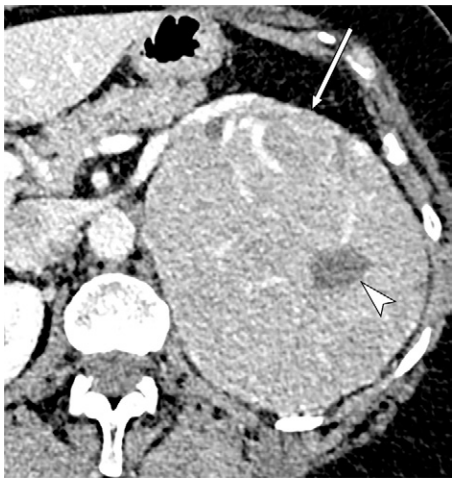

Figure 8. Left adrenal pheochromocytoma incidentally detected at coronary CT in a 67-year-old woman. Subsequent axial contrast-enhanced abdominal CT image shows a large left adrenal mass (arrow) with areas of central cystic change and/or necrosis (arrowhead). The well-circumscribed mass shows no invasion of adjacent structures. Pheochromocytoma was confirmed at resection.

At imaging, myelolipoma has predominantly macroscopic fat attenuation (less than −20 HU) on CT images or suppressed T1 hyperintensity on inversion-recovery or frequency-selective fat-suppression MR images (10,20). On opposed-phase chemical shift MR images, India ink artifact is present at the interface between normal adrenal tissue or soft-tissue components of a myelolipoma and the macroscopic fat (10,20). Myelolipoma is typically a well-circumscribed round or elliptical mass (59). The majority of adrenal myelolipomas demonstrate no or slow growth, with growth of greater than 1 cm associated with larger myelolipomas and hemorrhage (60). For patients who are symptomatic, often owing to larger myelolipomas, adrenalectomy should be considered (60).

As mentioned earlier, myelolipomatous degeneration within an adrenal mass (most commonly adenoma) should be considered in cases of nodules with small foci of macroscopic fat (26,28); this pathologic entity is often misinterpreted as myelolipoma. Because adenomas, including those with myelolipomatous degeneration, may be functional, hormonal evaluation may be warranted for patients who have an adenoma with myelolipomatous degeneration (26).

Bilateral Adrenal Myelolipomas in Congenital Adrenal Hyperplasia

Congenital adrenal hyperplasia results from 21-hydroxylase deficiency, and the absence of this enzyme disrupts the adrenal steroid biosynthesis pathway (61). The adrenal glands enlarge and sometimes develop multiple fat-containing masses owing to excessive adrenal cortical stimulation caused by adrenocorticotropic hormone (ACTH) (62). The majority of myelolipomas are unilateral; when they are bilateral, there is a strong correlation with congenital adrenal hyperplasia (Fig 11) (27).

Metastasis

Non–Fat-containing Metastasis

Metastases are the most common malignant adrenal tumor. However, adrenal incidentalomas are unlikely to represent metastases (2,3). Cancers of the lung, bowel, breast, and pancreas are the most common malignancies that metastasize to the adrenal gland (10). The imaging appearance of adrenal metastases is nonspecific, overlapping with that of other adrenal tumors (Fig 12).

At nonenhanced CT, adrenal metastases have an attenuation higher than 10 HU and typically do not wash out on postcontrast images (10). Similar to pheochromocytomas, metastases from clear cell RCC, HCC, melanoma, and neuroendocrine tumors are hypervascular (63) and may show washout. FDG PET/CT is both sensitive and specific in differentiating benign from malignant lesions.

ACC is characteristically a large, heterogeneous, enhancing mass (37,41) that has features that may be seen in metastasis (Fig 13). This carcinoma may be suggested in the absence of a primary extra-adrenal malignancy and in the presence of adrenocortical hormone excess and calcifications (37,41). Clues to the diagnosis of a metastasis include the presence or history of an extra-adrenal primary malignancy, bilateral or multifocal tumors, rapid growth, and interval development (4). Differentiating ACC from metastasis with imaging may be difficult but is imperative, as the surgical approach for ACC is adrenalectomy, while adrenal metastasis is most often treated systemically.

Fat-containing Metastasis

Rarely, metastases from microscopic fat–containing extra-adrenal malignancies can have microscopic fat (Fig 14), presenting

Figure 9. Left pheochromocytoma incidentally detected at CT in a 69-year-old man. Axial adrenal washout CT images obtained during the nonenhanced **(A)**, portal venous **(B)**, and 15-minute delayed **(C)** phases show a 2.6-cm left adrenal nodule (arrow) with attenuations of 49 HU, 100 HU, and 63 HU, respectively, and an absolute washout of 73%. Despite elevated metanephrine levels at biochemical evaluation, the patient underwent CT-guided fine-needle aspiration for unclear reasons, with pheochromocytoma confirmed at biopsy and resection. If there is clinical or biochemical suspicion for a pheochromocytoma, biopsy should not be performed, and surgical consultation is recommended.

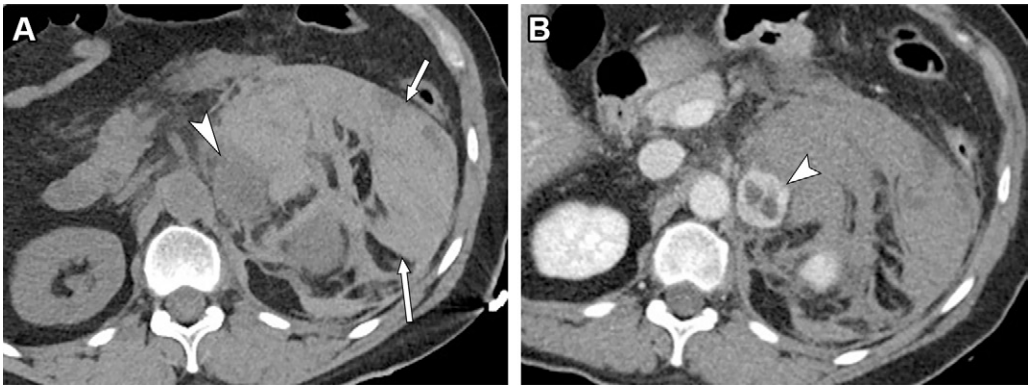

Figure 10. Pheochromocytoma with hemorrhage in a 68-year-old woman who had COVID-19 2 weeks earlier and presented with left flank pain and symptoms of hypotension. **(A)** Axial nonenhanced CT image shows a large left retroperitoneal hematoma (arrows) and left adrenal mass (arrowhead). **(B)** Axial portal venous phase CT image shows intense enhancement of the left adrenal mass (arrowhead) with central cystic-necrotic change.

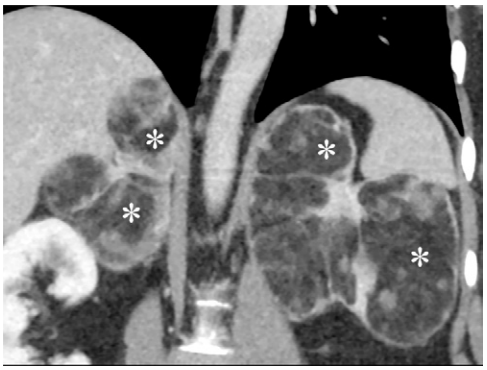

Figure 11. Bilateral myelolipomas in a 40-year-old patient with congenital adrenal hyperplasia due to 21-hydroxylase deficiency. The patient was born with ambiguous genitalia, was raised as female, and now identifies as male. Coronal portal venous phase CT image shows enlarged adrenal glands with multiple macroscopic fat-containing adrenal masses (*) measuring up to 13 cm on the left and up to 10 cm on the right. The size of the masses had increased markedly from 9 years earlier, from 9 cm on the left and 6 cm on the right (not shown), owing to noncompliance with the steroid treatment protocol.

a diagnostic dilemma because lipid-rich adenomas are diagnosed on the basis of the presence of microscopic fat. Such primary malignancies include clear cell RCC and HCC (64,65). Clues to the diagnosis of a fat-containing metastasis include presence or history of a primary malignancy with microscopic fat, a new adrenal mass, multiplicity, other metastases, and hypermetabolism on FDG PET/CT images (66). In addition, increased T2-weighted signal intensity and heterogeneity are features that can differentiate clear cell RCC metastasis from adenoma (20).

Bilateral Adrenal Abnormalities

Adrenal Hyperplasia

Adrenal hyperplasia is characterized by nonneoplastic enlargement of the adrenal glands. At imaging, this manifests as diffuse bilateral thickening with adreniform morphology (67). Occasionally, there is a micronodular or macronodular appearance. Rarely, hyperplasia is unilateral. There are multiple types of adrenal hyperplasia, depending on the inciting factor. A few examples include ACTH-dependent adrenal hyperplasia, adrenocortical nodular disease, and congenital adrenal hyperplasia (67).

ACTH-dependent Adrenal Hyperplasia.—The pituitary gland normally secretes ACTH to stimulate the adrenal glands to produce cortisol. Normally, elevated cortisol feeds back on the pituitary gland to decrease ACTH production. The decreased ACTH production, in turn, decreases cortisol production by the adrenal glands. Pituitary tumors that produce excess ACTH can cause adrenal hyperplasia because these hypersecreting tumors are unaffected by this feedback loop. Similarly, ectopic ACTH production in paraneoplastic syndromes can

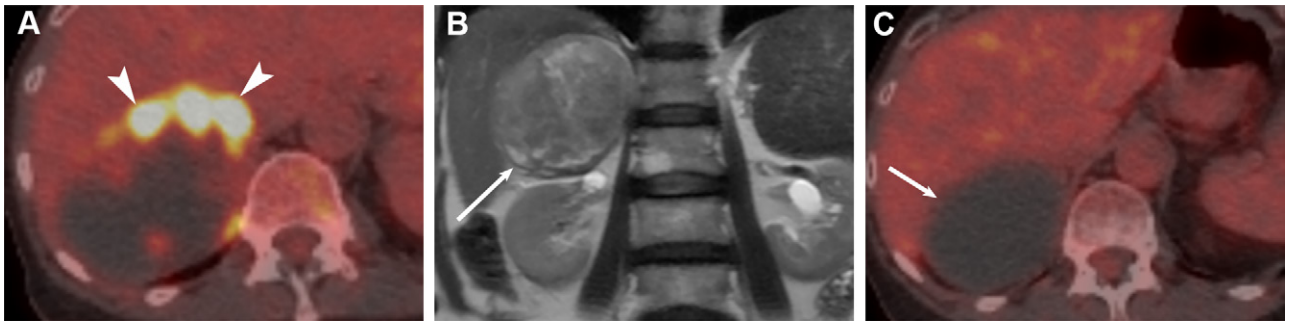

Figure 12. Right adrenal metastasis in a 76-year-old woman with non–small cell lung cancer. **(A)** Axial fused FDG PET/CT image shows areas of uptake along the periphery of a heterogeneous 7.5-cm right adrenal mass (arrowheads). **(B)** Coronal T2-weighted MR image shows a well-circumscribed heterogeneous predominantly T2-hyperintense mass (arrow). Microscopic fat was not present on in-phase and opposed-phase chemical-shift MR images (not shown), and there were no clinical or laboratory findings of pheochromocytoma. The differential diagnosis included metastasis, nonfunctioning pheochromocytoma, and ACC. The results of two biopsies were nondiagnostic. The adrenal lesion was treated as a metastasis. **(C)** Axial fused FDG PET/CT image after 6 months of treatment with an immune checkpoint inhibitor (pembrolizumab) shows response to treatment, with the adrenal mass (arrow) demonstrating a smaller size and no radiotracer uptake.

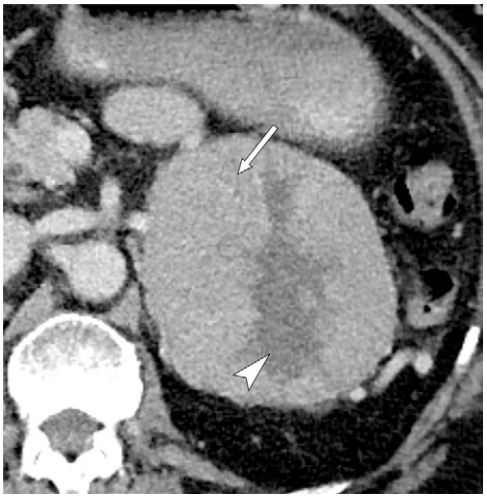

Figure 13. Left adrenal metastasis in a 64-year-old man with hepatitis C–related cirrhosis and HCC. The patient had undergone transarterial chemoembolization 1 month earlier. Axial contrast-enhanced portal venous phase CT image shows a large left adrenal mass with central hypoattenuation (arrowhead) and peripheral enhancement (arrow). Subsequent MRI findings (not shown) confirmed T2-hyperintense signal and nonenhancement of the central portion of the mass, compatible with necrosis.

result in adrenal hyperplasia that escapes the normal feedback mechanism. Nearly half of all of the ectopic ACTH production is from lung malignancies (67,68). Medullary thyroid carcinoma and malignancies arising from the thymus, bowel, and pancreas less commonly cause ectopic ACTH production. These tumors and their extra-adrenal metastases can cause adrenal hyperplasia, sometimes developing rapidly and mimicking adrenal metastasis. However, diffuse smooth enlargement of both adrenal glands with adreniform morphology is suggestive of hyperplasia (Fig 15), although it is similar in appearance to lymphoma.

Adrenocortical Nodular Disease.—The World Health Organization classifies adrenocortical nodular disease into three subtypes: *(a)* sporadic nodular, *(b)* bilateral micronodular, and *(c)* bilateral macronodular (53). The latter two entities are associated with germline mutations and are distinguished according to nodule size (<1 cm for micronodular, ≥1 cm for macronodular) and affected patient population (children and young adults for micronodular, adults for macronodular) (53). Bilateral macronodular adrenocortical disease (Fig 16) is a rare cause of bilateral adrenal nodules that can result in clinical hypercortisolism or mild autonomous cortisol secretion (previously subclinical hypercortisolism) (53,69). Images show marked diffuse thickening of both adrenal glands, with multiple bilateral nodules. Differential considerations include bilateral metastases or adenomas. Other less common causes of bilateral nodules include pheochromocytoma, congenital adrenal hyperplasia, Cushing disease, and secondary adrenal hyperplasia from ectopic ACTH production (69).

Lymphoma

Adrenal lymphoma is rare and may be primary (less common) or secondary (more common) (4). The most common adrenal lymphoma subtype is non-Hodgkin lymphoma. Adrenal lymphoma is frequently bilateral, with up to 75% of primary adrenal lymphomas involving both glands (70). It may occur as focal or multifocal adrenal masses, but it typically occurs as diffuse adrenal enlargement (70) from secondary lymphoma associated with lymphadenopathy and splenomegaly. At CT, these tumors have homogeneous soft-tissue attenuation with mild enhancement. At MRI, they are homogeneous with T1-hypointense or T1-isointense signal, T2-hyperintense signal, mild enhancement, and diffusion restriction (4,70). At FDG PET/CT, there is increased radiotracer uptake (Fig 17) (70).

Rare Adrenal Lesions

Hemangioma

Adrenal hemangioma is a benign mesenchymal neoplasm that arises from the endothelium of blood vessels. The two primary subtypes are capillary and cavernous, although the cavernous subtype is most common (49,71). Affected patients are typically 50–70 years of age, with a slight female predominance (71). Adrenal hemangioma is nonfunctioning and often

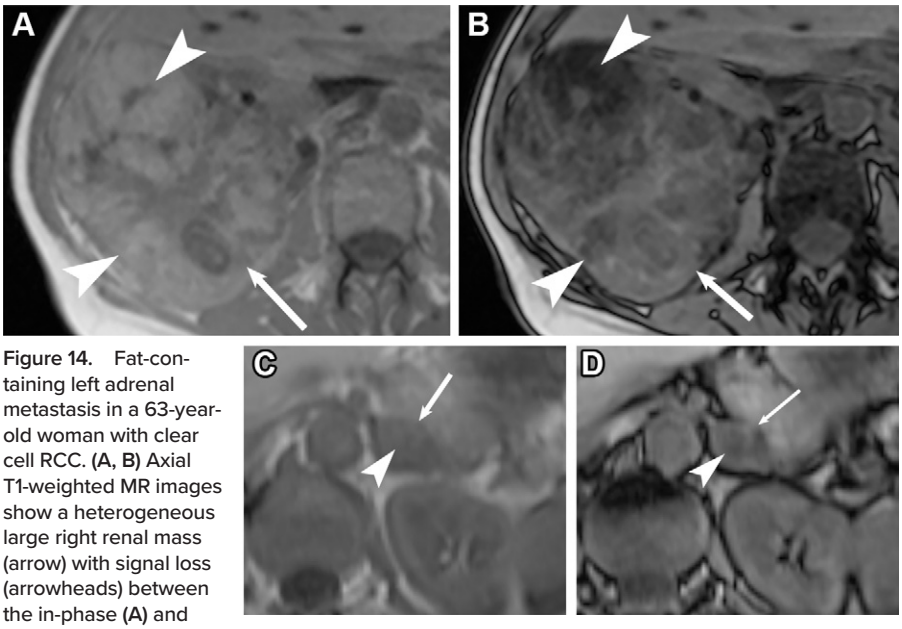

Figure 14. Fat-containing left adrenal metastasis in a 63-year-old woman with clear cell RCC. **(A, B)** Axial T1-weighted MR images show a heterogeneous large right renal mass (arrow) with signal loss (arrowheads) between the in-phase **(A)** and opposed-phase **(B)** sequences, indicating microscopic fat within a clear cell RCC. **(C, D)** Axial T1-weighted MR images of a 2.8-cm left adrenal nodule (arrow) show signal loss (arrowhead) between the in-phase **(C)** and opposed-phase **(D)** sequences, compatible with microscopic fat.

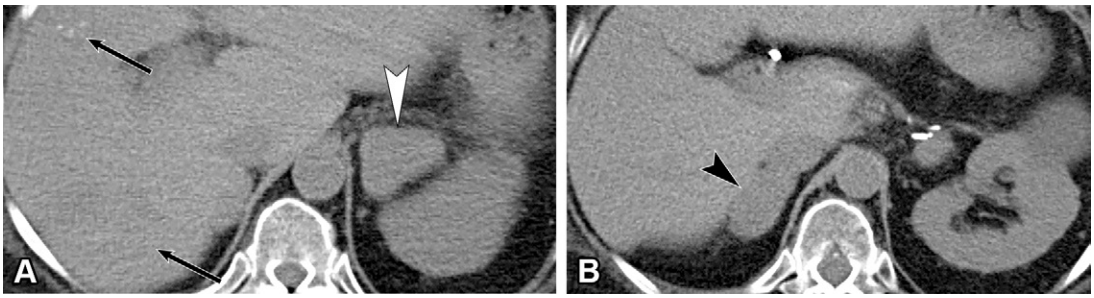

Figure 15. ACTH-producing pancreatic neuroendocrine tumor with metastases in a 58-year-old woman who was treated with partial pancreatectomy 14 years earlier, with recurrence of a 5.5-cm pancreatic mass (not shown). Nonenhanced CT images show multiple new and enlarging hepatic metastases (arrows in **A**), marked diffuse left adrenal thickening (arrowhead in **A**), and marked diffuse right adrenal thickening (arrowhead in **B**) with retention of the normal adrenal morphology. The adrenal glands were normal at CT performed 6 months earlier (not shown). These findings are compatible with bilateral adrenal hyperplasia secondary to progressive disease in the setting of an ACTH-producing primary malignancy.

incidentally detected (71). It is usually asymptomatic, but if it is larger than 10 cm, it may compress surrounding structures and cause abdominal pain. A known complication is rupture that results in retroperitoneal hemorrhage (71).

On CT images, hemangioma appears as a predominantly solid or mixed cystic and solid lesion with hypoattenuation centrally (41,49,71). Calcifications are common and favored to reflect phleboliths in dilated vascular spaces (71). At MRI, hemangioma is hyperintense on T2-weighted images and hypointense on T1-weighted images; focal areas of T1 and T2 hyperintensity indicate hemorrhage and necrosis (49,71). At both CT and MRI, adrenal hemangioma demonstrates peripheral discontinuous nodular enhancement during the arterial phase and progressive centripetal enhancement during postcontrast delayed phases (Fig 18) (41,49). It may be difficult to differentiate a hemangioma from other adrenal lesions if there is an absence of centripetal filling during postcontrast delayed phases (41). However, classic imaging features may suggest the possibility of hemangioma, and surveillance imaging may be an appropriate alternative to surgery.

Oncocytoma

With fewer than several hundred cases reported in the literature, adrenal oncocytoma (oncocytic adrenocortical adenoma or neoplasm) is a rare adrenal cortical tumor (4,72). This neoplasm is more predominant in women and occurs more frequently in the left adrenal gland (72). Most patients are asymptomatic.

At imaging, adrenal oncocytoma is often a large well-circumscribed tumor with mild heterogeneous enhancement (Fig S4). The mild enhancement and absence of lipid allow this lesion to be distinguished from pheochromocytoma and lipid-rich adrenal adenoma, respectively (4,72). While imaging cannot be used to distinguish benign from malignant adrenal oncocytic neoplasms, certain features have been associated with increased malignant potential. These features include

Figure 16. Bilateral macronodular adrenocortical disease in a 62-year-old man with long-standing poorly controlled hypertension. Axial nonenhanced CT image shows numerous bilateral adrenal nodules (arrows). Bilateral macronodular adrenocortical disease was confirmed at bilateral adrenalectomy.

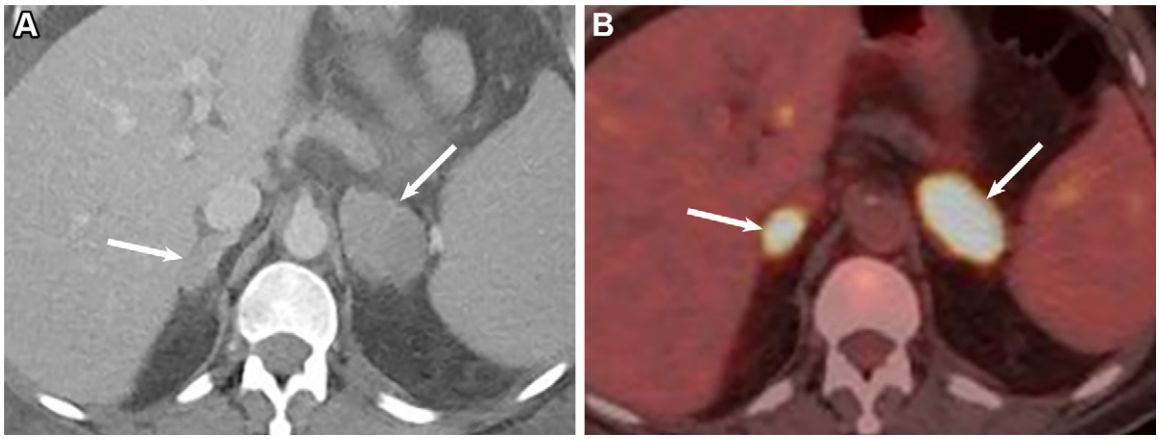

Figure 17. Bilateral adrenal lymphoma in a 67-year-old man with chronic lymphocytic leukemia and splenomegaly but no other sites of lymphoma seen at imaging. **(A)** Axial nonenhanced CT image shows homogeneous bilateral adrenal masses (arrows). **(B)** Fused FDG PET/CT image shows associated radiotracer uptake in the adrenal masses (arrows). Results of left adrenal gland biopsy confirmed diffuse large B-cell lymphoma.

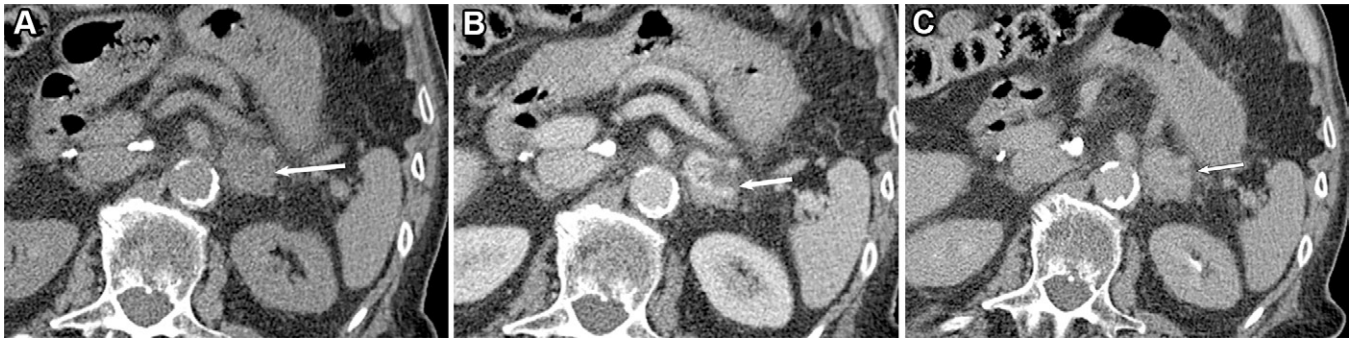

Figure 18. Incidental adrenal hemangioma in an 85-year-old woman. Dynamic axial CT images obtained in the nonenhanced **(A)**, arterial **(B)**, and delayed **(C)** phases show the classic hemangioma enhancement pattern: a left adrenal lesion (arrow) with peripheral discontinuous nodular enhancement during the arterial phase **(B)** and progressive contrast material fill-in during the postcontrast delayed phase **(C)**. The lesion was pathologically proved to be adrenal hemangioma after surgical resection.

more intense enhancement, size larger than 10 cm, vascular invasion, necrosis, and lymphadenopathy (4,72). Therefore, it may be difficult to differentiate malignant oncocytoma from pheochromocytoma. Adrenal oncocytomas are surgically resected.

Ganglioneuroma

Ganglioneuroma is a rare benign tumor comprised of ganglion and Schwann cells and arises along the sympathetic chain, including the adrenal medulla in 20%–30% of cases (49). Most patients are asymptomatic young adults (41,73).

On CT images, ganglioneuroma is homogeneously hypoattenuating (<40 HU) with mild progressive contrast enhancement (4). Stippled intralesional calcifications are common, occurring in roughly half of cases (41,49,73). Cystic change is uncommon (49).

At MRI, ganglioneuroma appears homogeneously or heterogeneously hyperintense on T2-weighted images and hypointense on T1-weighted images (Fig 19), probably secondary to ganglion cells and myxoid components. The interweaved bundles of collagen fibers and Schwann cells give a

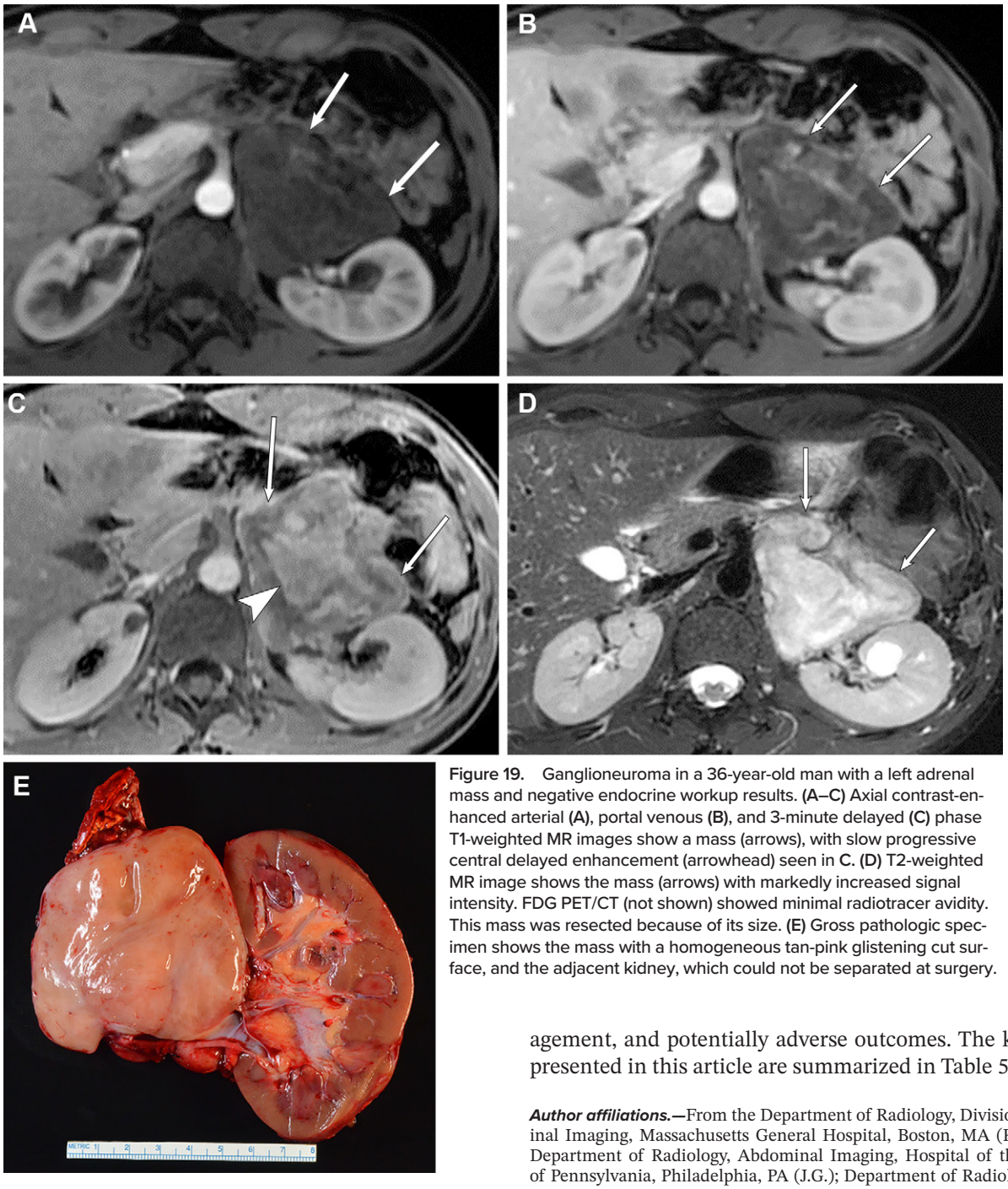

Figure 19. Ganglioneuroma in a 36-year-old man with a left adrenal mass and negative endocrine workup results. **(A–C)** Axial contrast-enhanced arterial **(A)**, portal venous **(B)**, and 3-minute delayed **(C)** phase T1-weighted MR images show a mass (arrows), with slow progressive central delayed enhancement (arrowhead) seen in **C**. **(D)** T2-weighted MR image shows the mass (arrows) with markedly increased signal intensity. FDG PET/CT (not shown) showed minimal radiotracer avidity. This mass was resected because of its size. **(E)** Gross pathologic specimen shows the mass with a homogeneous tan-pink glistening cut surface, and the adjacent kidney, which could not be separated at surgery.

whorled appearance on T2-weighted images (41,49). Dynamic contrast-enhanced MRI shows mild progressive enhancement (41,49). The average size of ganglioneuromas is 6–8 cm at diagnosis, and these neoplasms may be mistaken for ACC (73). In pediatric patients, the differential diagnosis includes neuroblastoma and ganglioneuroblastoma (4).

Conclusion

Atypical presentations of common benign and malignant adrenal masses, mimics of benign and malignant adrenal masses, and rare adrenal disease may pose diagnostic challenges for radiologists. Knowledge of clues to the correct diagnosis is needed to avoid misdiagnosis, suboptimal management, and potentially adverse outcomes. The key lessons presented in this article are summarized in Table 5.

Author affiliations.—From the Department of Radiology, Division of Abdominal Imaging, Massachusetts General Hospital, Boston, MA (R.C., M.A.B.); Department of Radiology, Abdominal Imaging, Hospital of the University of Pennsylvania, Philadelphia, PA (J.G.); Department of Radiology, Imaging Institute and Glickman Urological Institute, Cleveland Clinic, Cleveland, OH (E.M.R.); Department of Radiology, Mayo Clinic, Rochester, MN (P.N.); Department of Radiology, Center for Biomedical Imaging, NYU Grossman School of Medicine, NYU Langone Health, New York, NY (M.T.T.); Department of Radiology, Ohio State University Wexner Medical Center, Columbus, OH (C.E.H.); Department of Radiology, University of Alabama, Birmingham, AL (K.G.S.); Department of Diagnostic Imaging, University of Alberta, Edmonton, Alberta, Canada (W.T., G.L., M.B.); Departments of Radiology (B.W.C., M.T.C.) and Surgery (M.J.C.), UC Davis Medical Center, Sacramento, CA; Department of Radiology (J.T.L.), Department of General Surgery (C.Y.L.), and Department of Pathology and Laboratory Medicine (J.C.D.), University of Kentucky, Lexington, KY; Department of Diagnostic Radiology, University of Texas MD Anderson Cancer Center, 1515 Holcombe Blvd, Houston, TX 77030 (M.A.S., K.M.E.); Department of Radiology, University of Michigan, Ann Arbor, MI (E.M.C.); and Department of Radiology, University of Ottawa, Ottawa, Ontario, Canada (N.S.). Presented as an education exhibit at the 2021 RSNA Annual Meeting. Received September 27, 2022; revision requested November 9 and received December 21; accepted January 12, 2023. **Address correspondence to** K.M.E. (email: *kmelsayes@mdanderson.org*).

Table 5: Key Lessons for Diagnosis of Adrenal Neoplasms

Neoplasm	Tips
Adenoma	An adrenal nodule with homogeneous low attenuation (≤10 HU) on nonenhanced CT images and microscopic fat on chemical shift MR images is diagnostic of an adenoma Adrenal washout CT findings should not be stand-alone features for the diagnosis of lipid-poor adenoma; other features such as a mass size, heterogeneity, and clinical context should be considered to avoid misdiagnosis Adrenal washout CT is most useful for distinguishing adenoma from metastasis in patients with known nonhypervascular primary malignancy Heterogeneous signal loss within an adrenal mass at opposed-phase chemical shift MRI overwhelmingly represents microscopic fat within an adenoma in patients without and with malignancy.; however, one should be cautious in patients who have extra-adrenal malignancies with microscopic fat or when the heterogeneity may signify a collision tumor; follow-up imaging can be pursued in these settings While a mass >4 cm may represent an adenoma, a mass this size is generally resected because of the increased rate of malignancy; however, each patient should be managed individually by a multidisciplinary team
ACC	ACC rarely has attenuation <20 HU at nonenhanced CT and is most often >4 cm in size, with a heterogeneous appearance ACC often demonstrates absolute washout <60%; however, the washout may exceed 60%
Adrenal cysts	Endothelial cyst and pseudocyst make up the majority of adrenal cystic lesions Adrenal cyst may be confused for adenoma because of a nonenhanced attenuation of ≤10 HU and for pheochromocytoma with cystic and/or necrotic change, because of central hypoattenuation; however, it can be readily distinguished from the latter entities due to the absence of enhancement We do not recommend follow-up for adrenal cysts
Pheochromocytoma	Cystic and/or necrotic change within an adrenal mass should raise suspicion for pheochromocytoma An adrenal mass with a nonenhanced attenuation of ≤10 HU in the solid portion of the tumor rarely occurs with pheochromocytoma An adrenal mass with an absolute percentage washout of >60% may represent pheochromocytoma, particularly if there are other imaging or clinical features that suggest a hypervascular tumor with catecholamine excess; we recommend biochemical testing for pheochromocytoma when an adrenal mass demonstrates cystic and/or necrotic change or a portal venous phase attenuation of ≥130 HU, even if it demonstrates an absolute percent washout of >60% Biochemical assessment or molecular imaging may help distinguish pheochromocytoma from ACC; these neoplasms may have overlapping imaging features
Myelolipoma	Myelolipomas can be confidently diagnosed at imaging when fat makes up most of the mass An adrenal mass with a proportionally small focus of macroscopic fat should raise suspicion for myelolipomatous degeneration within an adrenal adenoma; because adenoma may be functional, one should consider hormonal evaluation when the possibility of adenoma with myelolipomatous degeneration is raised
Metastasis	Differentiating between ACC and adrenal metastasis is imperative, as ACC is treated with adrenalectomy, while adrenal metastasis is most often treated systemically Metastases from microscopic fat–containing extra-adrenal malignancies can have microscopic fat and mimic adenomas on opposed-phase chemical shift MR images; clues to the diagnosis of a fat-containing metastasis include presence or history of a primary malignancy with microscopic fat, development of a new adrenal mass, multiplicity, additional metastases, and hypermetabolism at FDG PET/CT
Bilateral adrenal lesions	Adrenal hyperplasia and adrenal lymphoma may be difficult to distinguish from one another, as both may present as diffuse bilateral adrenal enlargement or multifocal adrenal nodules; the presence of lymphadenopathy and splenomegaly is more suggestive of lymphoma
Rare adrenal lesions	The presence of classic imaging features of adrenal hemangioma (discontinuous peripheral nodular enhancement with progressive centripetal filling) may suggest the possibility of hemangioma, and surveillance imaging may be an appropriate alternative to surgery An adrenal mass with mild progressive enhancement may represent ganglioneuroma

***Disclosures of conflicts of interest.*—E.M.R.** Member of Society of Abdominal Radiology Board of Directors. **M.T.C.** Consulting fees from Corcept Therapeutics. **K.M.E.** Editorial board member of *RadioGraphics.* All other authors, the editor, and the reviewers have disclosed no relevant relationships.

References

1. Mayo-Smith WW, Song JH, Boland GL, et al. Management of Incidental Adrenal Masses: A White Paper of the ACR Incidental Findings Committee. J Am Coll Radiol 2017;14(8):1038–1044.
2. Kahramangil B, Kose E, Remer EM, et al. A Modern Assessment of Cancer Risk in Adrenal Incidentalomas: Analysis of 2219 Patients. Ann Surg 2022;275(1):e238–e244.
3. Song JH, Chaudhry FS, Mayo-Smith WW. The incidental adrenal mass on CT: prevalence of adrenal disease in 1,049 consecutive adrenal masses in patients with no known malignancy. AJR Am J Roentgenol 2008;190(5):1163–1168.
4. Lattin GE Jr, Sturgill ED, Tujo CA, et al. From the radiologic pathology archives: adrenal tumors and tumor-like conditions in the adult—radiologic-pathologic correlation. RadioGraphics 2014;34(3):805–829.
5. Boland GWL, Blake MA, Hahn PF, Mayo-Smith WW. Incidental adrenal lesions: principles, techniques, and algorithms for imaging characterization. Radiology 2008;249(3):756–775.
6. Kim YK, Park BK, Kim CK, Park SY. Adenoma characterization: adrenal protocol with dual-energy CT. Radiology 2013;267(1):155–163.
7. Botsikas D, Stefanelli S, Boudabbous S, Toso S, Becker CD, Montet X. Model-based iterative reconstruction versus adaptive statistical iterative

reconstruction in low-dose abdominal CT for urolithiasis. AJR Am J Roentgenol 2014;203(2):336–340.
8. Nagayama Y, Inoue T, Oda S, et al. Adrenal Adenomas versus Metastases: Diagnostic Performance of Dual-Energy Spectral CT Virtual Noncontrast Imaging and Iodine Maps. Radiology 2020;296(2):324–332.
9. Cao J, Lennartz S, Parakh A, et al. Dual-layer dual-energy CT for characterization of adrenal nodules: can virtual unenhanced images replace true unenhanced acquisitions? Abdom Radiol (NY) 2021;46(9):4345–4352.
10. Adam SZ, Nikolaidis P, Horowitz JM, et al. Chemical Shift MR Imaging of the Adrenal Gland: Principles, Pitfalls, and Applications. RadioGraphics 2016;36(2):414–432.
11. Corwin MT, Navarro SM, Malik DG, et al. Differences in Growth Rate on CT of Adrenal Adenomas and Malignant Adrenal Nodules. AJR Am J Roentgenol 2019;213(3):632–636.
12. Pantalone KM, Gopan T, Remer EM, et al. Change in adrenal mass size as a predictor of a malignant tumor. Endocr Pract 2010;16(4):577–587.
13. Haider MA, Ghai S, Jhaveri K, Lockwood G. Chemical shift MR imaging of hyperattenuating (>10 HU) adrenal masses: does it still have a role? Radiology 2004;231(3):711–716.
14. Israel GM, Korobkin M, Wang C, Hecht EN, Krinsky GA. Comparison of unenhanced CT and chemical shift MRI in evaluating lipid-rich adrenal adenomas. AJR Am J Roentgenol 2004;183(1):215–219.
15. Sebro R, Aslam R, Muglia VF, Wang ZJ, Westphalen AC. Low yield of chemical shift MRI for characterization of adrenal lesions with high attenuation density on unenhanced CT. Abdom Imaging 2015;40(2):318–326.
16. Caoili EM, Korobkin M, Francis IR, Cohan RH, Dunnick NR. Delayed enhanced CT of lipid-poor adrenal adenomas. AJR Am J Roentgenol 2000;175(5):1411–1415.
17. Caoili EM, Korobkin M, Francis IR, et al. Adrenal masses: characterization with combined unenhanced and delayed enhanced CT. Radiology 2002;222(3):629–633.
18. Corwin MT, Badawy M, Caoili EM, et al. Incidental Adrenal Nodules in Patients Without Known Malignancy: Prevalence of Malignancy and Utility of Washout CT for Characterization—A Multiinstitutional Study. AJR Am J Roentgenol 2022;219(5):804–812.
19. Chung R, O'Shea A, Sweeney AT, Mercaldo ND, McDermott S, Blake MA. Hereditary and Sporadic Pheochromocytoma: Comparison of Imaging, Clinical, and Laboratory Features. AJR Am J Roentgenol 2022;219(1):97–109.
20. Schieda N, Siegelman ES. Update on CT and MRI of Adrenal Nodules. AJR Am J Roentgenol 2017;208(6):1206–1217.
21. Corwin MT, Mitchell AS, Wilson M, Campbell MJ, Fananapazir G, Loehfelm TW. Accuracy of focal cystic appearance within adrenal nodules on contrast-enhanced CT to distinguish pheochromocytoma and malignant adrenal tumors from adenomas. Abdom Radiol (NY) 2021;46(6):2683–2689.
22. Boland GWL. Adrenal imaging. Abdom Imaging 2011;36(4):472–482.
23. He X, Peter PR, Auchus RJ. Approach to the Patient with an Incidental Adrenal Mass. Med Clin North Am 2021;105(6):1047–1063.
24. Schieda N, Davenport MS, Pedrosa I, et al. Renal and adrenal masses containing fat at MRI: proposed nomenclature by the society of abdominal radiology disease-focused panel on renal cell carcinoma. J Magn Reson Imaging 2019;49(4):917–926.
25. Rao P, Kenney PJ, Wagner BJ, Davidson AJ. Imaging and pathologic features of myelolipoma. RadioGraphics 1997;17(6):1373–1385.
26. Guccione J, Soliman M, Zhang M, et al. Imaging characteristics of pathologically proven adrenal adenomas with myelolipomatous degeneration: correlation with clinical and pathologic features. Br J Radiol 2022;95(1129):20210555.
27. Anbardar MH, Soleimani N, Nikeghbalian S, Mohebbi M. Adrenocortical adenoma with myelolipomatous metaplasia: a potential diagnostic pitfall: a case report and review of the literature. J Med Case Reports 2021;15(1):333.
28. Elbanan MG, Javadi S, Ganeshan D, et al. Adrenal cortical adenoma: current update, imaging features, atypical findings, and mimics. Abdom Radiol (NY) 2020;45(4):905–916.
29. Hammond NA, Lostumbo A, Adam SZ, et al. Imaging of adrenal and renal hemorrhage. Abdom Imaging 2015;40(7):2747–2760.
30. Rajiah P, Parakh A, Kay F, Baruah D, Kambadakone AR, Leng S. Update on Multienergy CT: Physics, Principles, and Applications. RadioGraphics 2020;40(5):1284–1308.
31. Badawy M, Gaballah AH, Ganeshan D, et al. Adrenal hemorrhage and hemorrhagic masses; diagnostic workup and imaging findings. Br J Radiol 2021;94(1127):20210753.
32. Panjawatanan P, Daniyal M, Delgado Hurtado J. Adrenal Mass Hemorrhage Clinically Mimicking a Pheochromocytoma. J Endocr Soc 2021;5(Supplement_1):A112.
33. Queiroz-Andrade M, Blasbalg R, Ortega CD, et al. MR imaging findings of iron overload. RadioGraphics 2009;29(6):1575–1589.
34. Thomas JP. Aldosterone deficiency in a patient with idiopathic haemochromatosis. Clin Endocrinol (Oxf) 1984;21(3):271–277.
35. Taffel M, Petrocelli RD, Rigau D, et al. Prevalence of Malignancy in Adrenal Nodules With Heterogeneous Microscopic Fat on Chemical-Shift MRI: A Multiinstitutional Study. AJR Am J Roentgenol 2023;220(1):86–94.
36. Newhouse JH, Heffess CS, Wagner BJ, Imray TJ, Adair CF, Davidson AJ. Large degenerated adrenal adenomas: radiologic-pathologic correlation. Radiology 1999;210(2):385–391.
37. Bharwani N, Rockall AG, Sahdev A, et al. Adrenocortical carcinoma: the range of appearances on CT and MRI. AJR Am J Roentgenol 2011;196(6):W706–W714.
38. Mantero F, Arnaldi G. Management approaches to adrenal incidentalomas. A view from Ancona, Italy. Endocrinol Metab Clin North Am 2000;29(1):107–125, ix.
39. Iñiguez-Ariza NM, Kohlenberg JD, Delivanis DA, et al. Clinical, Biochemical, and Radiological Characteristics of a Single-Center Retrospective Cohort of 705 Large Adrenal Tumors. Mayo Clin Proc Innov Qual Outcomes 2017;2(1):30-39.
40. Elhassan YS, Alahdab F, Prete A, et al. Natural History of Adrenal Incidentalomas With and Without Mild Autonomous Cortisol Excess: A Systematic Review and Meta-analysis. Ann Intern Med 2019;171(2):107–116.
41. Ahmed AA, Thomas AJ, Ganeshan DM, et al. Adrenal cortical carcinoma: pathology, genomics, prognosis, imaging features, and mimics with impact on management. Abdom Radiol (NY) 2020;45(4):945–963.
42. Dong A, Cui Y, Wang Y, Zuo C, Bai Y. (18)F-FDG PET/CT of adrenal lesions. AJR Am J Roentgenol 2014;203(2):245–252.
43. Berry R, Busireddy K, Chu LC, Johnson PT, Fishman EK. The good, the bad, and the ugly: uncommon CT appearances of pheochromocytoma. Abdom Radiol (NY) 2022;47(4):1406–1413.
44. Cyranska-Chyrek E, Szczepanek-Parulska E, Olejarz M, Ruchala M. Malignancy Risk and Hormonal Activity of Adrenal Incidentalomas in a Large Cohort of Patients from a Single Tertiary Reference Center. Int J Environ Res Public Health 2019;16(10):1872.
45. Lanoix J, Djelouah M, Chocardelle L, et al. Differentiation between heterogeneous adrenal adenoma and non-adenoma adrenal lesion with CT and MRI. Abdom Radiol (NY) 2022;47(3):1098–1111.
46. Ranathunga DS, Cherpak LA, Schieda N, Flood TA, McInnes MDF. Macroscopic Fat in Adrenocortical Carcinoma: A Systematic Review. AJR Am J Roentgenol 2020;214(2):390–394.
47. Rozenblit A, Morehouse HT, Amis ES Jr. Cystic adrenal lesions: CT features. Radiology 1996;201(2):541–548.
48. Ricci Z, Chernyak V, Hsu K, et al. Adrenal cysts: natural history by long-term imaging follow-up. AJR Am J Roentgenol 2013;201(5):1009–1016.
49. Wang MX, Mahmoud HS, Klimkowski S, et al. Cystic adrenal masses: spectrum of multimodality imaging features and pathological correlation. Clin Radiol 2022;77(7):479–488.
50. Borhani AA, Hosseinzadeh K. Quantitative Versus Qualitative Methods in Evaluation of T2 Signal Intensity to Improve Accuracy in Diagnosis of Pheochromocytoma. AJR Am J Roentgenol 2015;205(2):302–310.
51. Motta-Ramirez GA, Remer EM, Herts BR, Gill IS, Hamrahian AH. Comparison of CT findings in symptomatic and incidentally discovered pheochromocytomas. AJR Am J Roentgenol 2005;185(3):684–688.
52. Andreoni C, Krebs RK, Bruna PC, et al. Cystic phaeochromocytoma is a distinctive subgroup with special clinical, imaging and histological features that might mislead the diagnosis. BJU Int 2008;101(3):345–350.
53. Mete O, Erickson LA, Juhlin CC, et al. Overview of the 2022 WHO Classification of Adrenal Cortical Tumors. Endocr Pathol 2022;33(1):155–196.
54. Mohammed MF, ElBanna KY, Ferguson D, Harris A, Khosa F. Pheochromocytomas Versus Adenoma: Role of Venous Phase CT Enhancement. AJR Am J Roentgenol 2018;210(5):1073–1078.
55. Northcutt BG, Trakhtenbroit MA, Gomez EN, Fishman EK, Johnson PT. Adrenal Adenoma and Pheochromocytoma: Comparison of Multidetector CT Venous Enhancement Levels and Washout Characteristics. J Comput Assist Tomogr 2016;40(2):194–200.
56. Kang S, Oh YL, Park SY. Distinguishing pheochromocytoma from adrenal adenoma by using modified computed tomography criteria. Abdom Radiol (NY) 2021;46(3):1082–1090.
57. Taïeb D, Pacak K. Molecular imaging and theranostic approaches in pheochromocytoma and paraganglioma. Cell Tissue Res 2018;372(2):393–401.
58. Al-Bahri S, Tariq A, Lowentritt B, Nasrallah DV. Giant bilateral adrenal myelolipoma with congenital adrenal hyperplasia. Case Rep Surg 2014;2014:728198.
59. Decmann Á, Perge P, Tóth M, Igaz P. Adrenal myelolipoma: a comprehensive review. Endocrine 2018;59(1):7–15.
60. Hamidi O, Raman R, Lazik N, et al. Clinical course of adrenal myelolipoma: a long-term longitudinal follow-up study. Clin Endocrinol (Oxf) 2020;93(1):11–18.
61. Karaosmanoglu AD, Onder O, Leblebici CB, et al. Cross-sectional imaging features of unusual adrenal lesions: a radiopathological correlation. Abdom Radiol (NY) 2021;46(8):3974–3994.

62. Shaaban AM, Rezvani M, Tubay M, Elsayes KM, Woodward PJ, Menias CO. Fat-containing Retroperitoneal Lesions: Imaging Characteristics, Localization, and Differential Diagnosis. RadioGraphics 2016;36(3):710–734.
63. Nandra G, Duxbury O, Patel P, Patel JH, Patel N, Vlahos I. Technical and Interpretive Pitfalls in Adrenal Imaging. RadioGraphics 2020;40(4):1041–1060.
64. Sydow BD, Rosen MA, Siegelman ES. Intracellular lipid within metastatic hepatocellular carcinoma of the adrenal gland: a potential diagnostic pitfall of chemical shift imaging of the adrenal gland. AJR Am J Roentgenol 2006;187(5):W550–W551.
65. Shinozaki K, Yoshimitsu K, Honda H, et al. Metastatic adrenal tumor from clear-cell renal cell carcinoma: a pitfall of chemical shift MR imaging. Abdom Imaging 2001;26(4):439–442.
66. Tu W, Abreu-Gomez J, Udare A, Alrashed A, Schieda N. Utility of T2-weighted MRI to Differentiate Adrenal Metastases from Lipid-Poor Adrenal Adenomas. Radiol Imaging Cancer 2020;2(6):e200011.
67. Michelle MA, Jensen CT, Habra MA, et al. Adrenal cortical hyperplasia: diagnostic workup, subtypes, imaging features and mimics. B J Radiol 2017;90(1079):20170330.
68. Agrons MM, Jensen CT, Habra MA, et al. Adrenal cortical hyperplasia: diagnostic workup, subtypes, imaging features and mimics. Br J Radiol 2017;90(1079):20170330.
69. Bourdeau I, El Ghorayeb N, Gagnon N, Lacroix A. Management of endocrine disease: differential diagnosis, investigation and therapy of bilateral adrenal incidentalomas. Eur J Endocrinol 2018;179(2):R57–R67.
70. Leite NP, Kased N, Hanna RF, et al. Cross-sectional imaging of extranodal involvement in abdominopelvic lymphoproliferative malignancies. RadioGraphics 2007;27(6):1613–1634.
71. Arkadopoulos N, Kyriazi M, Yiallourou AI, et al. A rare coexistence of adrenal cavernous hemangioma with extramedullar hemopoietic tissue: a case report and brief review of the literature. World J Surg Oncol 2009;7(1):13.
72. Tirkes T, Gokaslan T, McCrea J, et al. Oncocytic neoplasms of the adrenal gland. AJR Am J Roentgenol 2011;196(3):592–596.
73. Elsayes KM, Elmohr MM, Javadi S, et al. Mimics, pitfalls, and misdiagnoses of adrenal masses on CT and MRI. Abdom Radiol (NY) 2020;45(4):982–1000.